

000 001 002 003 004 005 DOMED: REDESIGNING ENSEMBLE DISTILLATION 006 FOR DOMAIN GENERALIZATION 007 008 009

010 **Anonymous authors**
011 Paper under double-blind review
012
013
014
015
016
017
018
019
020
021
022
023
024
025
026
027

ABSTRACT

028 Domain generalization aims to improve model performance on unseen, out-of-
029 distribution (OOD) domains, yet existing methods often overlook the crucial aspect
030 of uncertainty quantification in their predictions. While ensemble learning com-
031 bined with knowledge distillation offers a promising avenue for enhancing both
032 model accuracy and uncertainty estimation without incurring significant compu-
033 tational overhead at inference time, this approach remains largely unexplored in
034 the context of domain generalization. In this work, we systematically investigate
035 different ensemble and distillation strategies for domain generalization tasks and
036 design a tailored data allocation scheme to enhance OOD generalization as well as
037 reduce computational cost. Our approach trains base models on distinct subsets
038 of domains and performs distillation on complementary subsets, thereby fostering
039 model diversity and training efficiency. Furthermore, we develop a novel tech-
040 nique that decouples uncertainty distillation from the standard distillation process,
041 enabling the accurate distillation of uncertainty estimation capabilities without
042 compromising model accuracy. Our proposed method, *Domain-aware Ensemble*
043 *Distillation* (DomED), is extensively evaluated against state-of-the-art domain
044 generalization and ensemble distillation techniques across multiple benchmarks,
045 achieving competitive accuracies and substantially improved uncertainty estimates.

046 1 INTRODUCTION

047 A fundamental assumption in many machine learning techniques is that training and test data are
048 drawn from the same distribution. However, this assumption often fails in real-world scenarios,
049 where models trained in one environment may be deployed in a different environment, leading to a
050 distributional shift. Domain generalization (DG) (Shankar et al., 2018; Zhou et al., 2020) addresses
051 this challenge by training a model on multiple source domains such that it can better generalize to
052 unseen target domains.

053 Existing DG methods primarily focus on learning domain-invariant representations, employing
054 techniques like explicit feature alignment (Ghifary et al., 2015; Maniyar et al., 2020), domain
055 adversarial learning (Du et al., 2021; Li et al., 2018b), and feature disentanglement (Mahajan
056 et al., 2021; Zhang et al., 2022). While effective, these methods still exhibit limited generalization
057 performance on out-of-distribution (OOD) data, often not significantly outperforming carefully-tuned
058 empirical risk minimization (ERM) (Gulrajani & Lopez-Paz, 2020). More critically, they tend to
059 produce overconfident yet erroneous predictions on OOD data (Ovadia et al., 2019), rendering their
060 predictions unreliable. This highlights the need to consider both prediction accuracy and uncertainty
061 estimation in developing robust DG methods.

062 Ensemble methods, which average the outputs of multiple models, are known to improve generaliza-
063 tion and provide more accurate uncertainty estimates (Opitz & Maclin, 1999; Dietterich, 2000; Zhou
064 et al., 2002; Rokach, 2010; Lakshminarayanan et al., 2017), particularly for epistemic uncertainty.
065 However, the computational and memory overhead of using ensembles at inference time can be
066 prohibitive. Knowledge distillation offers a solution by compressing an ensemble into a single,
067 efficient model while preserving its uncertainty estimation capabilities (Tran et al., 2020; Malinin
068 et al., 2019; Ferianc & Rodrigues, 2022). Recent work has explored self-distilling an ensemble of the
069 output logits from training data with the same label (Lee et al., 2022), but the potential of combining
070 explicit ensemble learning with uncertainty-aware distillation remains underexplored in the context
071 of DG. Specifically, a principled framework for leveraging domain labels to construct diverse experts

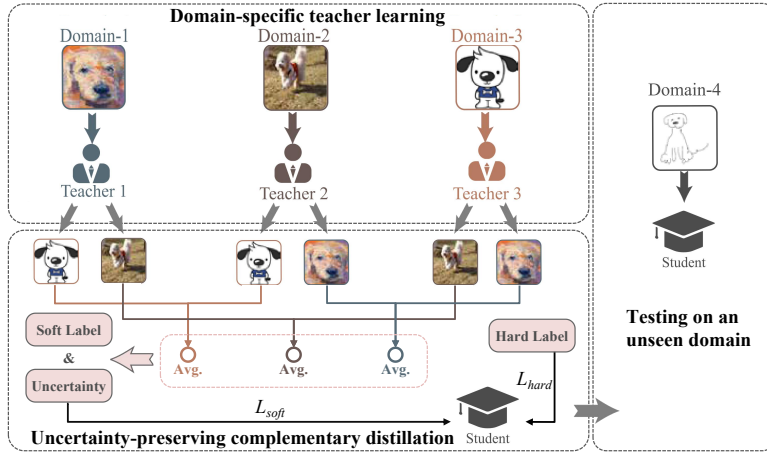


Figure 1: Illustration of DomED. Each teacher model is trained on a specific source domain. The teachers collectively make predictions on data complementary to their respective training data, such that their generalization ability along with their inherent uncertainty information can be distilled to a student model. After distillation, the student model is evaluated on a previously unseen target domain.

remains elusive, and simultaneously preserving prediction and uncertainty estimation capabilities presents a non-trivial optimization conflict (Ryabinin et al., 2021).

In this work, we aim to develop a tailored ensemble learning and knowledge distillation scheme for domain generalization. Although it is not fully understood how ensemble learning improves the test-time performance of deep neural networks, recent work suggests that training multiple models to exploit the “multi-view” structure in data is crucial for the success of ensemble methods (Allen-Zhu & Li, 2020). This aligns with the understanding that model diversity is key in ensemble learning (Brown et al., 2005; Nam et al., 2021a). Unlike regular classification tasks, DG provides domain labels for each data sample, presenting a natural opportunity for multi-view learning. We propose to train the base models of an ensemble on different, non-overlapping subsets of domains. This enhances model diversity while reducing the training cost of individual models. We then evaluate and compare different data allocation schemes for ensembling and distillation to identify the optimal scheme. To the best of our knowledge, we are the first to systematically investigate the possible data allocation schemes for adapting ensemble distillation to the particular setting of domain generalization.

Beyond achieving high accuracy on unseen domains, our goal is to distill the uncertainty estimation capability of ensembles. A common approach is to train a prior network to output a conjugate prior (e.g., a Dirichlet distribution for classification tasks) that captures the output distributions of the base models (Malinin & Gales, 2018; Malinin et al., 2019). However, we find that this approach significantly degrades model accuracy in DG compared to standard distillation (Hinton et al., 2015). To address this, we introduce a novel technique that decouples uncertainty distillation from standard distillation, allowing for accurate model predictions and uncertainty estimates simultaneously. We refer to our approach as *Domain-aware Ensemble Distillation* (DomED), as illustrated in Figure 1.

Our main contributions are summarized as follows:

- We explore tailored ensemble and distillation strategies for domain generalization tasks, and develop a novel data allocation scheme that trains and distills base models on complementary domains, which enhances model diversity and training efficiency.
- We identify that the commonly used uncertainty distillation method degrades the accuracy of an ensemble after distillation in the context of DG. We address this by proposing a decoupled distillation technique that preserves both mean prediction accuracy and model uncertainty.
- We conduct extensive experiments to compare different data allocation schemes and evaluate our approach, DomED, on multiple domain generalization benchmarks. Our results demonstrate that DomED achieves competitive accuracies and significantly improved uncertainty quantification compared to existing methods.

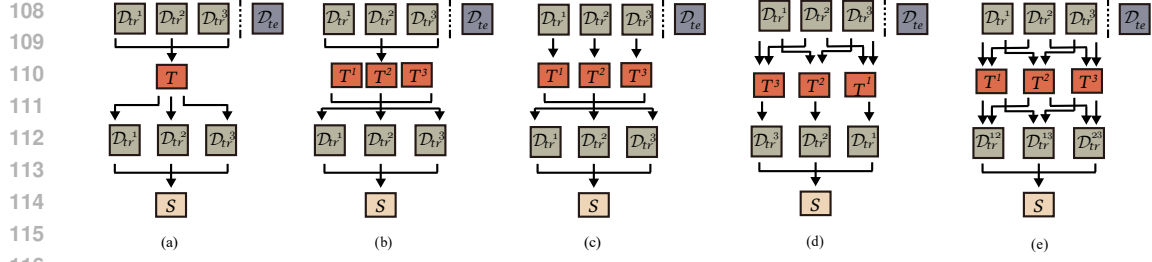


Figure 2: Comparison of different data allocation schemes for ensemble learning and knowledge distillation. Note that these are different from the DomED scheme presented in Figure 1. Given M training domains, (a) self-distillation from a single teacher model; (b) standard ensemble distillation (all teachers trained and distilled on all domains); (c) includes M single-domain teachers, distilled on all domains; (d) includes M teachers, each trained on $M-1$ domains and distilled on the remaining domain; and (e) includes M teachers, each trained and distilled on the same $M-1$ domains.

2 METHODS

We present our ensemble learning and knowledge distillation methods for domain generalization. First, we formally define the domain generalization problem and introduce the relevant notation. We then discuss various ensembling and distillation strategies and develop a tailored scheme for domain generalization that achieves high model accuracy and reduced training cost. Based on this scheme, we further propose a novel uncertainty-preserving distillation method, which decouples uncertainty distillation from the standard distillation process, to simultaneously achieve accurate model predictions and uncertainty estimates.

2.1 PROBLEM DEFINITION

We consider a domain generalization problem with M source domains (training domains), whose union is denoted as $\mathcal{D}_{tr} = \bigcup_{m=1}^M \mathcal{D}_{tr}^m$, and one unseen target domain (test domain), \mathcal{D}_{te} . Each source domain, \mathcal{D}_{tr}^m , contains N_m independent and identically distributed (i.i.d.) labeled training samples, i.e., $\mathcal{D}_{tr}^m := \{(x_i^m, y_i^m)\}_{i=1}^{N_m}$. Similarly, the target domain comprises N_{te} unlabeled i.i.d. samples, $\mathcal{D}_{te} := \{x_j\}_{j=1}^{N_{te}}$. While all domains share a common feature space \mathcal{X} and label space \mathcal{Y} , the core challenge is that the data distribution varies across domains. In image classification, for instance, domains might represent different visual styles (e.g., photos, sketches) but share the same set of object categories. The objective is to learn a function $f: \mathcal{X} \rightarrow \mathcal{Y}$ using only data from the source domains that can effectively generalize to the unseen target domain.

2.2 ENSEMBLE AND DISTILLATION STRATEGIES

In a regular supervised learning problem that has i.i.d. data for both training and testing, the base models of an ensemble are usually trained on the same dataset, and model diversity is introduced only by the independent initialization of their parameters (Allen-Zhu & Li, 2020). Moreover, the distillation of the ensemble is also done on the same set of training data. In contrast, a domain generalization task splits data into multiple domains, making it possible to increase model diversity by training base models on different subsets of domains. Furthermore, for each base model, it is also possible to use a different set of data than its training data for distillation. As shown in Figure 1 and Figure 2, we consider six representative training data allocation schemes, and compare them empirically in Section 3. Among them, Figure 2(a) depicts the self-distillation scheme, and Figure 2(b) depicts the regular ensembling and distillation scheme. For fair comparison, we assume an ensemble of M base models (one for each source domain), $\{T^m\}_{m=1}^M$. In this section, we discuss in detail the scheme employed by DomED (as shown in Figure 1) due to its superior empirical performance and relatively low computational cost. In the following, we also refer to the base models of an ensemble and the distilled model, respectively, as teacher models and student model.

Domain-specific teacher models. The data allocation scheme of DomED is designed to maximize teacher diversity by training each of the M teacher models on a single, distinct source domain. This strategy treats each domain as a unique “view” of the data, encouraging the models to develop different specializations. Specifically, each teacher model, T^m , is a neural network parameterized by weights θ_T^m and is trained exclusively on its corresponding domain, \mathcal{D}_{tr}^m . The complete set of

teacher parameters is denoted as $\theta_T = \{\theta_T^m\}_{m=1}^M$. For classification tasks, each teacher is trained to minimize the cross-entropy loss on its respective domain:

$$\mathcal{L}_T^m = \mathbb{E}_{(x_i^m, y_i^m) \in \mathcal{D}_{tr}^m} [\text{CE}(\pi(x_i^m; \theta_T^m), y_i^m)], \quad (1)$$

where $\text{CE}(\cdot, \cdot)$ denotes the cross-entropy between two categorical distributions, y_i^m denotes the ground-truth label of x_i^m , and $\pi(x_i^m; \theta_T^m)$ represents the predictive distribution output by the teacher.

A key advantage of this domain-specific training scheme is its computational efficiency. While training M teachers may seem costly, the total computational cost can be significantly less than training a single model on all source domains. This is because each domain-specific teacher can be trained with a smaller batch size (e.g. $1/M$) and requires significantly fewer training steps to become an effective guide for distillation. Crucially, as detailed in Appendix A.1, we empirically find that the student model’s performance saturates even before the individual teachers have fully converged, substantially reducing the training overhead that typically makes ensemble methods impractical.

Complementary Distillation. As illustrated in Figure 1, DomED employs a complementary distillation strategy designed to transfer the generalization ability of the teacher models to the student. The core principle is to generate distillation targets for samples from a given source domain, \mathcal{D}_{tr}^m , using only the teachers that were never trained on it. Specifically, for an input sample $x_i^m \in \mathcal{D}_{tr}^m$, we first gather the output logits $z^n(x_i^m)$ from all complementary teachers T^n (where $n \neq m$). These logits are then aggregated by averaging to produce a single soft target for distillation:

$$\bar{z}(x_i^m) = \frac{1}{M-1} \sum_{\substack{n=1 \\ n \neq m}}^M z^n(x_i^m). \quad (2)$$

The student model is then trained to emulate these aggregated predictions by minimizing a temperature-scaled cross-entropy loss. For each source domain \mathcal{D}_{tr}^m , this soft-target loss is defined as:

$$\mathcal{L}_{\text{soft}}^m = \mathbb{E}_{(x_i^m, \cdot) \in \mathcal{D}_{tr}^m} [\text{CE}(\pi(x_i^m; \theta_S), \bar{\pi}(x_i^m; \theta_T, \tau^m))], \quad (3)$$

where $\pi(x_i^m; \theta_S)$ is the distribution predicted by the student model, and $\bar{\pi}(x_i^m; \theta_T, \tau^m)$ is the distribution derived from the aggregated logits $\bar{z}(x_i^m)$ by applying the softmax function with a temperature hyperparameter τ^m . τ^m is usually set between 1 and 4, and a larger τ produces a softer probability distribution. Note that $\bar{\pi}(x_i^m; \theta_T, \tau^m)$ does not receive gradient and θ_T does not update during distillation. This complementary distillation is also employed in the data allocation scheme shown in Figure 2(d).

As a common practice for knowledge distillation (Hinton et al., 2015), the student model is also trained on the ground-truth labels to achieve higher model accuracy. Similar to the loss in Eq. 1, we minimize the following cross-entropy loss:

$$\mathcal{L}_{\text{hard}}^m = \mathbb{E}_{(x_i^m, y_i^m) \in \mathcal{D}_{tr}^m} [\text{CE}(\pi(x_i^m; \theta_S), y_i^m)]. \quad (4)$$

Finally, the two losses in Eqs. 3 and 4 are combined as the training loss of student model:

$$\mathcal{L}_S = \frac{1}{M} \sum_{m=1}^M [\lambda \mathcal{L}_{\text{soft}}^m + (1 - \lambda) \mathcal{L}_{\text{hard}}^m], \quad (5)$$

where λ is a hyperparameter that balances the soft and hard targets. See Appendix F.1 for more details on tuning λ .

2.3 UNCERTAINTY-PRESERVING DISTILLATION

While the distillation scheme discussed in Section 2.2 produces an accurate student model, it discards the ensemble’s valuable epistemic uncertainty. This limitation is inherent to the standard cross-entropy objective, which trains the student to match only the *mean* of the teacher predictions. In doing so, it collapses the full predictive distribution into a single point estimate, losing the diversity across teacher outputs that signals model uncertainty. To preserve this crucial information, we distill the ensemble’s uncertainty by training the student model to output the parameters of a Dirichlet prior.

216 **Learning a Dirichlet Prior.** The Dirichlet distribution is the conjugate prior of the categorical
 217 distribution, making it well-suited for modeling the predictive uncertainty of an ensemble. It provides
 218 a principled way to represent a distribution over distributions, which naturally captures the set of
 219 predictions from the teacher models.

220 Given C classes, the Dirichlet distribution is defined by its positive concentration parameters $\alpha =$
 221 $[\alpha_1, \dots, \alpha_C]$. The sum of these parameters, $\alpha_0 = \sum_{c=1}^C \alpha_c$, is known as the precision of the
 222 distribution; a higher precision indicates lower uncertainty (a more peaked distribution). The
 223 probability density function (PDF) is given by:
 224

$$225 \quad \text{Dir}(\pi; \alpha) = \frac{\Gamma(\alpha_0)}{\prod_{c=1}^C \Gamma(\alpha_c)} \prod_{c=1}^C (\pi_c)^{\alpha_c - 1}, \quad (6)$$

228 where π is a probability vector. To enable a student model to output this distribution, we parameterize
 229 the concentration parameters from its logits, $z_c(x_i^m)$, for an input x_i^m as $\alpha_c(x_i^m) = e^{z_c(x_i^m)}$. The
 230 student is then trained to find the Dirichlet parameters that best explain the collection of teacher
 231 predictions by minimizing the following negative log-likelihood (NLL) loss (Malinin et al., 2019):
 232

$$233 \quad \mathcal{L}_{\text{Dir}} = \mathbb{E}_{(x_i^m, \cdot) \in \mathcal{D}_{tr}^m} \left[\sum_{c=1}^C \ln \Gamma(\alpha_c(x_i^m)) - \ln \Gamma(\alpha_0(x_i^m)) \right. \\ 234 \quad \left. - \frac{1}{M-1} \sum_{n=1}^M \sum_{\substack{c=1 \\ n \neq m}}^C (\alpha_c(x_i^m) - 1) \ln \pi_c(x_i^m; \theta_T^n) \right], \quad (7)$$

238 where $\pi_c(x_i^m; \theta_T^n)$ is the probability assigned to class c by teacher T^n .
 239

240 **Decoupled Uncertainty Distillation.** While directly minimizing the Dirichlet NLL loss (\mathcal{L}_{Dir}) is a
 241 common approach for uncertainty distillation (Malinin & Gales, 2018; Malinin et al., 2019), we find
 242 that it can degrade accuracy in the challenging context of domain generalization. This issue arises
 243 because \mathcal{L}_{Dir} implicitly attempts to solve two coupled problems simultaneously: matching the *mean*
 244 of the ensemble’s predictions and matching their *spread* (i.e., uncertainty). As noted by Ryabinin
 245 et al. (2021), these objectives can conflict, forcing the model to compromise on accuracy to better fit
 246 the uncertainty.

247 To resolve this, we propose decoupling these objectives by assigning a specialized loss to each task:
 248

- 249 a) We use the standard distillation loss, \mathcal{L}_S , to distill the mean prediction. This cross-entropy-
 250 based loss is highly effective at aligning the student with the teachers’ mean prediction, thereby
 251 preserving model accuracy.
- 252 b) We use the Dirichlet NLL loss, \mathcal{L}_{Dir} , to capture the uncertainty of the ensemble’s predictions.
 253 When teachers agree, the target Dirichlet distribution is sharp, teaching the student to be confident.
 254 When they disagree, the distribution is flat, teaching the student to reflect this uncertainty.

255 By combining them, we use the dominant \mathcal{L}_S loss to enforce an accurate mean prediction, while \mathcal{L}_{Dir}
 256 focuses on its primary strength: shaping the predictive uncertainty around that mean. This leads to
 257 our final, decoupled objective:
 258

$$259 \quad \mathcal{L}'_S = \mathcal{L}_S + \beta \mathcal{L}_{\text{Dir}}, \quad (8)$$

260 where β is a hyperparameter balancing the two terms. In practice, we set β to a small value (e.g., 0.01),
 261 effectively using \mathcal{L}_{Dir} as a regularizer that fine-tunes the model’s uncertainty without disrupting the
 262 primary accuracy signal from \mathcal{L}_S . As we show in our analyses of the loss components (Appendices E
 263 and H) and the impact of β on convergence (Appendix F.2), this conceptually simple decoupling
 264 successfully preserves accuracy while enabling robust uncertainty transfer.

265 3 EXPERIMENTS

266 Our experiments systematically evaluate DomED on several domain generalization benchmarks.
 267 We first systematically compare the performance of six data allocation schemes proposed in this
 268 work. We then benchmark DomED against state-of-the-art methods on DomainBed and assess its
 269 uncertainty quantification performance using standard metrics. In addition, we present an ablation
 270 study of the distillation loss in Appendix E, and verify the architectural robustness of DomED in
 271 Appendix I.

Table 1: Comparison of different training data allocation schemes for ensemble learning and knowledge distillation. The best and second-best results indicated by bold and underlined, respectively.

Dataset	Domain	ERM	DomED (w/o dist.)	Scheme (a)	Scheme (b)	Scheme (c)	Scheme (d)	Scheme (e)	DomED (ours)
PACS	<i>Art Painting</i>	84.8 \pm 0.2	78.2 \pm 2.8	85.9 \pm 0.5	86.2 \pm 1.3	87.2 \pm 0.5	<u>87.5</u> \pm 0.8	85.9 \pm 0.6	87.5 \pm 0.5
	<i>Cartoon</i>	80.0 \pm 0.6	69.2 \pm 1.0	81.7 \pm 0.7	80.4 \pm 0.8	81.0 \pm 0.6	82.1 \pm 0.5	80.1 \pm 0.7	<u>81.5</u> \pm 0.3
	<i>Photo</i>	96.2 \pm 0.0	95.0 \pm 0.2	96.9 \pm 0.3	96.7 \pm 0.2	<u>97.0</u> \pm 0.2	96.5 \pm 0.8	96.4 \pm 0.2	97.1 \pm 0.2
	<i>Sketch</i>	79.3 \pm 0.3	68.6 \pm 4.8	79.7 \pm 0.4	79.1 \pm 1.1	<u>81.4</u> \pm 0.4	80.6 \pm 0.2	77.3 \pm 0.8	81.6 \pm 0.4
Avg.		85.1 \pm 0.2	77.7 \pm 0.9	86.1 \pm 0.4	85.6 \pm 0.4	86.6 \pm 0.3	<u>86.7</u> \pm 0.2	84.9 \pm 0.3	86.9 \pm 0.2
Office Home	<i>Art</i>	61.3 \pm 0.3	64.6 \pm 0.4	67.2 \pm 0.5	67.3 \pm 0.6	67.5 \pm 0.2	<u>67.6</u> \pm 0.2	67.4 \pm 0.3	67.7 \pm 0.1
	<i>Clipart</i>	52.1 \pm 0.4	52.1 \pm 0.2	56.4 \pm 0.6	56.4 \pm 0.6	56.7 \pm 0.3	<u>56.9</u> \pm 0.2	56.7 \pm 0.3	57.1 \pm 0.2
	<i>Product</i>	76.6 \pm 0.3	75.6 \pm 0.3	77.7 \pm 0.2	77.6 \pm 0.3	<u>78.1</u> \pm 0.2	78.0 \pm 0.2	77.7 \pm 0.1	78.2 \pm 0.2
	<i>RealWorld</i>	78.5 \pm 0.2	79.1 \pm 0.2	81.3 \pm 0.1	81.5 \pm 0.2	<u>81.7</u> \pm 0.1	81.6 \pm 0.1	81.2 \pm 0.1	81.8 \pm 0.1
Avg.		67.1 \pm 0.2	67.8 \pm 0.2	70.6 \pm 0.3	70.6 \pm 0.4	<u>71.0</u> \pm 0.2	<u>71.0</u> \pm 0.1	70.7 \pm 0.2	71.2 \pm 0.2
VLCS	<i>Caltech101</i>	97.8 \pm 0.1	93.8 \pm 3.7	98.2 \pm 0.3	98.3 \pm 0.3	98.5 \pm 0.2	98.2 \pm 0.1	97.8 \pm 0.4	98.5 \pm 0.1
	<i>LabelMe</i>	64.2 \pm 0.3	58.0 \pm 1.5	<u>65.4</u> \pm 0.4	65.5 \pm 0.5	64.8 \pm 0.3	64.9 \pm 0.2	63.6 \pm 0.4	65.3 \pm 0.2
	<i>SUN09</i>	72.6 \pm 0.4	77.0 \pm 0.9	73.3 \pm 0.9	74.8 \pm 0.4	78.0 \pm 0.2	78.8 \pm 0.2	72.9 \pm 0.3	<u>78.4</u> \pm 0.3
	<i>VOC2007</i>	77.6 \pm 0.4	76.7 \pm 1.5	77.3 \pm 0.4	77.7 \pm 0.3	78.9 \pm 0.2	77.8 \pm 0.1	77.2 \pm 0.4	<u>78.4</u> \pm 0.2
Avg.		78.0 \pm 0.3	76.4 \pm 1.7	78.5 \pm 0.5	79.1 \pm 0.3	80.1 \pm 0.2	79.9 \pm 0.1	77.9 \pm 0.4	80.1 \pm 0.1

3.1 EXPERIMENTAL SETUP

Datasets and evaluation protocol. We use the following datasets in our experiments: 1) PACS (Li et al., 2017), a widely used multi-source domain generalization dataset comprising 9,991 images across 7 classes and 4 domains (Art_painting, Cartoon, Photo, and Sketch), 2) Office-Home (Venkateswara et al., 2017), a dataset of 15,500 images from 65 classes and 4 domains (Art, Clipart, Product, and Real World), 3) VLCS (Fang et al., 2013), which contains 10,729 images of 5 classes sourced from Caltech101, LabelMe, SUN09, and VOC 2007, 4) TerraIncognita (Beery et al., 2018), a slightly larger dataset of 24,788 images from 10 classes and 4 domains, and 5) DomainNet (Peng et al., 2019), a significantly larger dataset of 586,575 images from 345 classes and 6 domains. Following the evaluation protocol of DomainBed (Gulrajani & Lopez-Paz, 2020), we perform leave-one-domain-out evaluation and use training-domain validation for hyperparameter tuning. In Tables 1 and 2, the reported accuracies are the average of 7 runs.

Implementation Details. To ensure a fair comparison, we follow the standard protocol of DomainBed (Gulrajani & Lopez-Paz, 2020) for all experiments. We use a pre-trained ResNet-50 (He et al., 2016) backbone. For the PACS, TerraIncognita, and DomainNet datasets, we use the Adam optimizer (Kingma & Ba, 2014) with a learning rate of 5×10^{-5} . For OfficeHome and VLCS, we use stochastic gradient descent (SGD) with an initial learning rate of 2×10^{-2} and a momentum of 0.9. Other hyperparameters, such as batch size, dropout rate, and weight decay, are adopted from recent state-of-the-art methods (Cha et al., 2021; 2022).

3.2 DOMAIN GENERALIZATION

Data allocation schemes. In addition to the complementary data allocation scheme illustrated in Figure 1, we investigate five other schemes as shown in Figure 2. Among them, scheme (a) is simple self-distillation without ensembling, scheme (b) corresponds to regular ensembling and distillation that use the full training data for both purposes, and the other three can be considered as variants of DomED. Compared to DomED, scheme (c) distills from all teachers regardless of their training domains, scheme (d) allocates each teacher $M - 1$ training domains instead of 1 but also distills on complementary domains, whereas scheme (e) distills on the respective training domains of teachers.

We evaluate the six data allocation schemes along with two baselines, ERM and DomED without distillation, on PACS, OfficeHome, and VLCS. The results are shown in Table 1. Comparing schemes (b) and (c), the latter achieves better accuracies on all three datasets, which suggests that training base models on different subsets of domains can indeed lead to better generalization, possibly due to increased model diversity. By comparing DomED with scheme (c), we also observe that

324 Table 2: Classification accuracy (%) on the DomainBed benchmark. Methods are grouped into
 325 standalone approaches and those using weight averaging. Best and second-best results in each group
 326 are in **bold** and underlined, respectively. “TerraInc.” stands for TerraIncognita. [†]Results reported
 327 by Gulrajani & Lopez-Paz (2020). [‡]Results reported by Di Zhao et al. (2025). [§]Test-time ensembling.
 328 [¶]Weight averaging from 60 runs.

Method	PACS	OfficeHome	VLCS	TerraInc.	DomainNet	Avg.
ERM (Vapnik, 1999)	85.1±0.2	67.1±0.2	78.0±0.3	47.8±0.6	44.0±0.1	64.4
CORAL [†] (Sun & Saenko, 2016)	86.2±0.3	68.7±0.3	78.8±0.6	47.6±1.0	41.5±0.1	64.5
DANN [†] (Ganin et al., 2016)	83.6±0.4	65.9±0.6	78.6±0.4	46.7±0.5	38.3±0.1	62.6
MMD [†] (Li et al., 2018b)	84.7±0.5	66.3±0.1	77.5±0.9	42.2±1.6	23.4±9.5	58.8
IRM [†] (Arjovsky et al., 2019)	83.5±0.8	64.3±2.2	78.5±0.5	47.6±0.8	33.9±2.8	61.1
Fish (Shi et al., 2021)	85.5±0.3	68.6±0.4	77.8±0.3	45.1±1.3	42.7±0.2	63.9
SagNet [†] (Nam et al., 2021b)	86.3±0.2	68.1±0.1	77.8±0.5	48.6±1.0	40.3±0.1	64.2
SelfReg (Kim et al., 2021)	85.6±0.4	67.9±0.7	77.8±0.9	47.0±0.3	42.8±0.1	64.2
NKD [‡] (Wang et al., 2021)	83.3±0.4	71.1±0.3	77.1±0.3	37.2±0.3	42.4±0.2	62.2
MIRO (Cha et al., 2022)	85.4±0.4	70.5±0.4	79.0±0.0	50.4±1.1	44.3±0.2	65.9
KDDRL (Niu et al., 2023)	86.6±0.8	66.9±1.6	77.3±0.5	48.0±1.1	38.5±0.3	63.4
SAGM (Wang et al., 2023b)	86.6±0.2	70.1±0.2	<u>80.0</u> ±0.3	48.8±0.9	45.0±0.2	66.1
DomainDrop (Guo et al., 2023)	87.9 ±0.3	68.7±0.1	79.8±0.3	51.5 ±0.4	44.4±0.5	<u>66.5</u>
RISE [‡] (Huang et al., 2023)	85.0±0.3	71.5±0.2	77.6±0.2	39.0±0.3	45.2±0.2	63.7
GMDG (Tan et al., 2024)	85.6±0.3	70.7±0.2	79.2±0.3	<u>51.1</u> ±0.9	44.6±0.1	66.3
XDomainMix (Liu et al., 2024)	86.4±0.4	-	-	48.2±1.3	44.4±0.2	-
Arith (Wang et al., 2025)	86.5±0.3	69.4±0.1	79.4±0.3	48.1±1.2	41.5±0.1	65.0
GGA (Ballas & Diou, 2025)	86.4±0.5	67.0±0.3	78.7±0.8	48.5±1.1	44.4±0.2	65.0
BOLD [‡] (Di Zhao et al., 2025)	85.7±0.2	72.6 ±0.2	78.7±0.2	44.3±0.3	46.9 ±0.2	65.6
DomED (ours)	<u>86.9</u> ±0.2	<u>71.2</u> ±0.2	80.1 ±0.1	50.2±0.5	<u>45.7</u> ±0.1	66.8
SWAD (Cha et al., 2021)	88.1±0.1	70.6±0.2	79.1±0.1	50.0±0.3	46.5±0.1	66.9
CORAL (w/ SWAD) (Cha et al., 2021)	88.3±0.1	71.3±0.1	<u>78.9</u> ±0.1	<u>51.0</u> ±0.1	46.8±0.0	67.3
SAM (w/ SWAD) (Cha et al., 2021)	87.1±0.2	69.9±0.2	78.5±0.1	45.3±0.9	46.5±0.1	65.5
DNA (w/ SWAD) (Chu et al., 2022)	88.4±0.1	71.2±0.1	79.0±0.1	<u>52.2</u> ±0.4	<u>47.2</u> ±0.1	67.6
EoA [§] (Arpit et al., 2022)	<u>88.6</u>	72.5	79.1	52.3	47.4	68.0
DiWA [¶] (Rame et al., 2022)	89.0	<u>71.6</u>	<u>79.4</u>	49.0	46.3	67.1
DomED (w/ SWAD) (ours)	88.4±0.2	<u>71.6</u> ±0.2	80.2 ±0.1	51.9±0.3	46.7±0.2	67.8

356 complementary distillation achieves comparable or slightly better accuracies than distillation on all
 357 domains, thus corroborating the intuition that DomED can distill the generalization ability into student
 358 model. Moreover, despite their similar classification performance, DomED outperforms scheme (c)
 359 in terms of uncertainty quantification (see Table 3). In contrast, distillation only on training domains
 360 (scheme (e)) can result in significantly worse accuracies compared to complementary distillation
 361 (scheme (d)). Furthermore, while both DomED and scheme (d) employ complementary distillation
 362 with comparable accuracies, DomED restricts each teacher to a single domain. This design minimizes
 363 training overhead while maximizing model diversity (see Appendix B.1), a prerequisite for robust
 364 uncertainty quantification. Finally, we note that the teacher models of DomED are relatively weak
 365 as each individual model is trained on only one domain; thus, they perform poorly compared to the
 366 distilled model. Nevertheless, the distilled model proves to be resilient even when individual teachers
 367 are trained on scarce data, mitigating the risk of negative transfer (see Appendix C). Collectively, the
 368 systematic evaluation confirms that our data allocation strategy is a principled and effective design
 369 choice for achieving high teacher diversity and robust distillation.

370 **Results on DomainBed.** We evaluate DomED on the DomainBed benchmark against a wide array
 371 of state-of-the-art methods, with results presented in Table 2. To provide a clear comparison, we group
 372 methods into standard approaches and those that utilize weight averaging techniques like SWAD
 373 to further boost performance. As a standalone method, DomED demonstrates strong performance,
 374 achieving significant gains over the ERM baseline: +1.8 pp on PACS, +4.1 pp on OfficeHome,
 375 +2.1 pp on VLCS, +2.4 pp on TerraIncognita, and +1.7 pp on DomainNet. The improvement is
 376 particularly pronounced on OfficeHome, a dataset known for its large inter-domain gap. This setting
 377 is ideal for our approach, as it allows domain-specific teachers to become highly specialized, and
 378 our complementary distillation can then effectively integrate their diverse knowledge to improve
 379 generalization. When paired with SWAD, our method achieves a top-tier average accuracy of 67.8%,

378 which is highly competitive with other leading methods that employ significantly more computation,
 379 such as EoA (test-time ensembling) and DiWA (weight averaging from 60 runs). This highlights the
 380 efficiency of our approach, which delivers state-of-the-art performance without significant overhead.
 381 See Appendix A for a detailed analysis of computational cost.

383 3.3 UNCERTAINTY QUANTIFICATION

384 Beyond strong generalization performance, a crucial advantage of DomED is its ability to provide
 385 reliable uncertainty estimates. To evaluate this, we employ four standard metrics: mean classification
 386 error (ERR), prediction rejection ratio (PRR) (Malinin et al., 2019), expected calibration error
 387 (ECE) (Guo et al., 2017), and negative log-likelihood (NLL). A high PRR is desirable, as it indicates
 388 the model can effectively detect and reject its own incorrect predictions. A low ECE signifies
 389 well-calibrated confidence. They both are essential for trustworthy OOD generalization.

390 **Calibration and Reliability Analysis.** We con-
 391 duct a detailed analysis on the PACS dataset, com-
 392 paring DomED to various baselines. For reference,
 393 we also include two full test-time ensembles: a
 394 standard ensemble (3 base models) and an EoA en-
 395 semble (Arpit et al., 2022). The results are shown
 396 in Table 3 (see Appendix J for more detailed re-
 397 sults). Standard methods like ERM and CORAL
 398 achieve reasonable accuracy but are poorly cali-
 399 brated, evidenced by high ECE and NLL values.
 400 The poor calibration stems from a rapid entropy
 401 collapse during training, whereas the distillation
 402 process of DomED retains the dark knowledge
 403 from diverse teacher models, resulting in high-
 404 entropy predictions (see Appendix D). Post-hoc
 405 temperature scaling (Guo et al., 2017) improves
 406 calibration but fails to enhance the model’s abil-
 407 ity to reject incorrect predictions (PRR). Approx-
 408 imate Bayesian methods like MC Dropout (Gal
 409 & Ghahramani, 2016), which require multiple for-
 410 ward passes at inference, prove ineffective in this
 411 DG context, degrading accuracy without improv-
 412 ing calibration. Furthermore, EnD², while de-
 413 signed for uncertainty distillation, performs poorly
 414 due to the absence of ground-truth labels in the
 415 distillation process. In contrast, DomED strikes an
 416 exceptional balance between accuracy and cali-
 417 bration. See Appendix G for a comparison with more
 418 calibration strategies. The analysis highlights two
 419 key aspects of its design. First, the raw ‘DomED
 420 Teachers’ ensemble performs poorly on its own,
 421 confirming that our distillation process is essential
 422 to effectively integrate the specialists’ knowledge.

423 Second, DomED outperforms alternative distillation schemes (c) and (d) across all metrics, demon-
 424 strating the superiority of the complementary distillation strategy. Overall, DomED achieves the best
 425 performance among all single-inference methods. Crucially, while test-time ensembles serve as a
 426 strong performance ceiling, the competitive performance of DomED demonstrates the efficacy of our
 427 distillation strategy in transferring the benefits of an ensemble into a single efficient model. Finally,
 428 we present additional results on the impact of teacher diversity on model performance in Appendix B.

429 **Out-of-Distribution Detection.** We further assess the utility of DomED’s uncertainty estimates
 430 for out-of-distribution (OOD) detection. Following Malinin et al. (2019), we treat samples from the
 431 unseen test domain as OOD and samples from the source domains as in-distribution (ID). We use the
 432 area under the receiver operating characteristic curve (ROC-AUC) to measure the model’s ability to
 433 distinguish between these two groups using total uncertainty and knowledge uncertainty. As shown in
 434 Table 4 (see Appendix J for more detailed results), DomED’s OOD detection performance is highly
 435 competitive with that of a full test-time ensemble (3 base models). On average, it closely matches the

383 Table 3: Uncertainty quantification performance
 384 on PACS. DomED is the best single-inference
 385 method.

Model	ERR↓	ECE↓	NLL↓	PRR↑
Ensemble	0.130	0.038	0.471	0.798
EoA	0.114	0.058	0.403	0.837
ERM	0.149	0.089	0.625	0.776
Temp. Scaling	0.147	0.048	0.487	0.773
MC Drop (p=0.5)	0.175	0.129	0.873	0.746
MC Drop (p=0.1)	0.157	0.112	0.755	0.769
CORAL	0.138	0.082	0.586	0.598
EnD ²	0.326	0.220	1.580	0.084
DomED Teachers	0.281	0.148	1.063	0.536
Scheme (c)	0.134	0.054	0.502	0.751
Scheme (d)	0.133	0.091	0.523	0.743
DomED (Ours)	0.131	0.044	0.473	0.787

383 Table 4: ROC-AUC of OOD detection. T.Unc
 384 and K.Unc refer to total and knowledge uncer-
 385 tainty, respectively.

Models	PACS		OfficeHome	
	T.Unc	K.Unc	T.Unc	K.Unc
ERM	0.71	—	0.67	—
Ensemble	0.73	0.71	0.69	0.70
DomED	0.71	0.72	0.60	0.70

Models	VLCS		TerraIncognita	
	T.Unc	K.Unc	T.Unc	K.Unc
ERM	0.51	—	0.75	—
Ensemble	0.53	0.54	0.78	0.79
DomED	0.57	0.69	0.77	0.75

432 ensemble’s ability to identify novel, unseen domains, which is crucial for safe and reliable real-world
 433 deployment.
 434

435 4 RELATED WORK 436

437 4.1 DOMAIN GENERALIZATION 438

439 Domain Generalization (DG) addresses the challenge of dataset shift (Moreno-Torres et al., 2012),
 440 where a model’s performance degrades when training and testing distributions differ. Existing
 441 DG methods are often categorized into three main groups (Wang et al., 2022): data manipulation,
 442 representation learning, and learning strategies. Data manipulation methods augment training data
 443 to enhance diversity and quantity (Volpi et al., 2018; Zhou et al., 2021). Representation learning
 444 aims to find domain-invariant features, often through feature alignment or disentanglement (Du et al.,
 445 2021; Mahajan et al., 2021; Zhang et al., 2022; Dayal et al., 2024). Recent work in this area has
 446 explored finer-grained control, such as by suppressing domain-sensitive channels (Guo et al., 2023) or
 447 establishing more general objectives for invariant features (Tan et al., 2024). Finally, various learning
 448 strategies adapt existing machine learning techniques for DG, including ensemble learning (Arpit
 449 et al., 2022; Lee et al., 2022; Niu et al., 2023), meta-learning (Li et al., 2018a; Guan et al., 2023;
 450 Chen et al., 2023; Wang et al., 2025), and gradient operations (Shi et al., 2021; Ballas & Diou, 2025).
 451

452 4.2 ENSEMBLE METHODS AND DISTILLATION 453

454 Ensemble methods have proven effective in improving OOD generalization. For instance, Arpit et al.
 455 (2022) employs an ensemble of moving average models to achieve better generalization performance,
 456 which, however, relies on costly test-time ensembling that incurs significant inference overhead.
 457 To avoid test-time ensembling, efficient fusion techniques have also been developed, including
 458 knowledge distillation (Hinton et al., 2015), weight averaging (Cha et al., 2021; Chu et al., 2022;
 459 Rame et al., 2022), and model merging (Ding et al., 2025). In the context of domain generalization,
 460 knowledge distillation can be enhanced by gradient regularization (Wang et al., 2021) or combined
 461 with language guidance (Huang et al., 2023). Apart from full-model ensembling, parameter-efficient
 462 expert aggregation has also attracted attention. For instance, AdapterFusion (Pfeiffer et al., 2021)
 463 leverages knowledge from multiple tasks by training and fusing task-specific adapters, and recent
 464 approaches focus on merging Low-Rank Adaptation (LoRA) modules (Hu et al., 2022) with minimal
 465 interference (Yadav et al., 2023). In contrast to these parameter-space techniques that primarily
 466 focus on accuracy, DomED operates in the output space to explicitly transfer both generalization
 467 capabilities and epistemic uncertainty.
 468

469 Theoretical work has shown that given the “multi-view” structure of data, an ensemble of inde-
 470 pendently trained neural networks can provably improve test accuracy, and such capability can be
 471 provably distilled into a single model (Allen-Zhu & Li, 2020). For domain generalization, Zhou
 472 et al. (2021) introduce domain adaptive ensemble learning, which encompasses a shared CNN feature
 473 extractor and multiple classifier heads, each excelling in one specific domain. In a similar vein, Niu
 474 et al. (2023) also use a shared feature extractor with multiple domain-specific heads, followed by a
 475 two-stage distillation scheme. However, the complex scheme yields only marginal gains on domain
 476 generalization tasks. Furthermore, Di Zhao et al. (2025) apply the idea of domain-specific experts to
 477 distillation from large pretrained models. Yao et al. (2023) propose to dynamically weight domain-
 478 specific models based on domain relations during inference. Other unconventional approaches
 479 include ensembling logits with the same label but from different domains (Lee et al., 2022) and
 480 ensembling meta-source models (Yan & Guo, 2025), though the latter leverages test-time batch
 481 statistics, positioning it closer to test-time adaptation than pure domain generalization. In addition,
 482 ensemble distillation has been utilized for out-of-distribution (OOD) detection (Wang et al., 2023a),
 483 a different focus than generalization to unseen domains. Despite this body of work, a systematic
 484 study of how the data allocation scheme for ensemble learning and distillation can be tailored to the
 485 specific setting of domain generalization has been largely overlooked.
 486

487 4.3 UNCERTAINTY ESTIMATION 488

489 In machine learning applications, distinguishing between data (aleatoric) uncertainty and model (epi-
 490 temic) uncertainty is essential to understand the decisions or predictions made by models (Gal, 2016).
 491 Ensemble methods are particularly effective at separating and quantifying these two types of uncer-
 492

tainty (Lakshminarayanan et al., 2017). An intuitive approach to uncertainty quantification (Hüllermeier & Waegeman, 2021; Depeweg et al., 2017) is to first derive the total uncertainty as the entropy of the expected predictive distribution for a data point (x, y) , i.e. $U_{tot} = \mathcal{H}(\mathbb{E}_{p(\theta|\mathcal{D})}[p_\theta(y|x)])$, where θ denotes model parameters, and \mathcal{D} represents the training data. Similarly, data uncertainty can be defined as the expected entropy of the predictive distribution of individual models, i.e. $U_{ale} = \mathbb{E}_{p(\theta|\mathcal{D})}[\mathcal{H}(p_\theta(y|x))]$; and model uncertainty can be naturally defined as $U_{tot} - U_{ale}$.

The Dirichlet distribution plays a crucial role in uncertainty quantification for classification models, particularly when distilling the knowledge of an ensemble into a single, efficient student model. As the conjugate prior of the categorical distribution, it provides a principled way to model a distribution over predicted probabilities. This approach is central to methods like Dirichlet prior networks (Tsiligkaridis, 2021; Malinin & Gales, 2018; Malinin et al., 2019) and evidential learning (Joo et al., 2020; Dawood et al., 2023; Schreck et al., 2024). However, training a model by directly minimizing the Dirichlet negative log-likelihood (NLL) can be problematic, as the loss function often degrades model accuracy in the process of improving uncertainty estimates (Ryabinin et al., 2021).

5 CONCLUSION

In this work, we introduced DomED, a redesigned ensemble distillation framework for domain generalization that jointly addresses model accuracy and uncertainty quantification. By combining a specialized data allocation strategy to enhance teacher diversity with a novel technique for decoupling mean and uncertainty distillation, DomED successfully transfers the knowledge of an ensemble into a single, efficient model. Our extensive experiments demonstrate that DomED achieves competitive accuracy while providing uncertainty estimates that rival a full, computationally expensive ensemble, underscoring the importance and feasibility of jointly optimizing for both objectives.

While our approach is more efficient than standard ensembling, its computational cost remains a limitation compared to single-model training, presenting a clear direction for future work on improving efficiency. Furthermore, the core principle of decoupled uncertainty distillation is broadly applicable. Extending this framework to other tasks, such as uncertainty-aware regression or dense prediction, is an exciting avenue for future research. Overall, this work provides a robust and practical foundation for building more reliable and uncertainty-aware models for domain generalization.

REFERENCES

Zeyuan Allen-Zhu and Yuanzhi Li. Towards understanding ensemble, knowledge distillation and self-distillation in deep learning. *arXiv preprint arXiv:2012.09816*, 2020.

Martin Arjovsky, Léon Bottou, Ishaan Gulrajani, and David Lopez-Paz. Invariant risk minimization. *arXiv preprint arXiv:1907.02893*, 2019.

Devansh Arpit, Huan Wang, Yingbo Zhou, and Caiming Xiong. Ensemble of averages: Improving model selection and boosting performance in domain generalization. *Advances in Neural Information Processing Systems*, 35:8265–8277, 2022.

Aristotelis Ballas and Christos Diou. Gradient-guided annealing for domain generalization. In *Proceedings of the Computer Vision and Pattern Recognition Conference*, pp. 20558–20568, 2025.

Sara Beery, Grant Van Horn, and Pietro Perona. Recognition in terra incognita. In *Proceedings of the European conference on computer vision (ECCV)*, pp. 456–473, 2018.

Gavin Brown, Jeremy Wyatt, Rachel Harris, and Xin Yao. Diversity creation methods: a survey and categorisation. *Information fusion*, 6(1):5–20, 2005.

Junbum Cha, Sanghyuk Chun, Kyungjae Lee, Han-Cheol Cho, Seunghyun Park, Yunsung Lee, and Sungrae Park. Swad: Domain generalization by seeking flat minima. *Advances in Neural Information Processing Systems*, 34:22405–22418, 2021.

Junbum Cha, Kyungjae Lee, Sungrae Park, and Sanghyuk Chun. Domain generalization by mutual-information regularization with pre-trained models. In *European Conference on Computer Vision*, pp. 440–457. Springer, 2022.

540 Jin Chen, Zhi Gao, Xinxiao Wu, and Jiebo Luo. Meta-causal learning for single domain generalization.
 541 In *Proceedings of the IEEE/CVF Conference on Computer Vision and Pattern Recognition*, pp.
 542 7683–7692, 2023.

543

544 Xu Chu, Yujie Jin, Wenwu Zhu, Yasha Wang, Xin Wang, Shanghang Zhang, and Hong Mei. Dna:
 545 Domain generalization with diversified neural averaging. In *International conference on machine
 546 learning*, pp. 4010–4034. PMLR, 2022.

547 Tareen Dawood, Emily Chan, Reza Razavi, Andrew P King, and Esther Puyol-Antón. Addressing
 548 deep learning model calibration using evidential neural networks and uncertainty-aware training.
 549 In *2023 IEEE 20th International Symposium on Biomedical Imaging (ISBI)*, pp. 1–5. IEEE, 2023.

550

551 Aveen Dayal, Vimal KB, Linga Reddy Cenkeramaddi, C Mohan, Abhinav Kumar, and Vineeth
 552 N Balasubramanian. Madg: margin-based adversarial learning for domain generalization. *Advances
 553 in Neural Information Processing Systems*, 36, 2024.

554 Stefan Depeweg, José Miguel Hernández-Lobato, Finale Doshi-Velez, and Steffen Udluft. Decompo-
 555 sition of uncertainty for active learning and reliable reinforcement learning in stochastic systems.
 556 *stat*, 1050:11, 2017.

557

558 Jingfeng Zhang Di Zhao, Hongsheng Hu, Philippe Fournier-Viger, Gillian Dobbie, and Yun Sing
 559 Koh. Balancing invariant and specific knowledge for domain generalization with online knowledge
 560 distillation. In *Proceedings of the Thirty-Fourth International Joint Conference on Artificial
 561 Intelligence, IJCAI-25*, pp. 2440–2448, 2025.

562 Thomas G Dietterich. Ensemble methods in machine learning. In *International workshop on multiple
 563 classifier systems*, pp. 1–15. Springer, 2000.

564

565 Yuhe Ding, Jian Liang, Bo Jiang, Zi Wang, Aihua Zheng, and Bin Luo. Harmonizing and merging
 566 source models for clip-based domain generalization. *arXiv preprint arXiv:2506.09446*, 2025.

567

568 Alexey Dosovitskiy, Lucas Beyer, Alexander Kolesnikov, Dirk Weissenborn, Xiaohua Zhai, Thomas
 569 Unterthiner, Mostafa Dehghani, Matthias Minderer, Georg Heigold, Sylvain Gelly, Jakob Uszkoreit,
 570 and Neil Houlsby. An image is worth 16x16 words: Transformers for image recognition at scale.
ICLR, 2021.

571

572 Yuntao Du, Jindong Wang, Wenjie Feng, Sinno Pan, Tao Qin, Renjun Xu, and Chongjun Wang.
 573 Adarnn: Adaptive learning and forecasting of time series. In *Proceedings of the 30th ACM
 574 international conference on information & knowledge management*, pp. 402–411, 2021.

575

576 Chen Fang, Ye Xu, and Daniel N Rockmore. Unbiased metric learning: On the utilization of multiple
 577 datasets and web images for softening bias. In *Proceedings of the IEEE International Conference
 578 on Computer Vision*, pp. 1657–1664, 2013.

579

580 Martin Ferianc and Miguel Rodrigues. Simple regularisation for uncertainty-aware knowledge
 581 distillation. *arXiv preprint arXiv:2205.09526*, 2022.

582

583 Yarin Gal. *Uncertainty in Deep Learning*. PhD thesis, University of Cambridge, 2016.

584

585 Yarin Gal and Zoubin Ghahramani. Dropout as a bayesian approximation: Representing model
 586 uncertainty in deep learning. In *international conference on machine learning*, pp. 1050–1059.
 587 PMLR, 2016.

588

589 Yaroslav Ganin, Evgeniya Ustinova, Hana Ajakan, Pascal Germain, Hugo Larochelle, François
 590 Laviolette, Mario March, and Victor Lempitsky. Domain-adversarial training of neural networks.
 591 *Journal of machine learning research*, 17(59):1–35, 2016.

592

593 Muhammad Ghifary, W Bastiaan Kleijn, Mengjie Zhang, and David Balduzzi. Domain generalization
 594 for object recognition with multi-task autoencoders. In *Proceedings of the IEEE international
 595 conference on computer vision*, pp. 2551–2559, 2015.

596

597 Zeli Guan, Yawen Li, Zhenhui Pan, Yuxin Liu, and Zhe Xue. Rfdg: Reinforcement federated domain
 598 generalization. *IEEE Transactions on Knowledge and Data Engineering*, 2023.

594 Ishaan Gulrajani and David Lopez-Paz. In search of lost domain generalization. *arXiv preprint*
595 *arXiv:2007.01434*, 2020.

596

597 Chuan Guo, Geoff Pleiss, Yu Sun, and Kilian Q Weinberger. On calibration of modern neural
598 networks. In *International conference on machine learning*, pp. 1321–1330. PMLR, 2017.

599

600 Jintao Guo, Lei Qi, and Yinghuan Shi. Domaindrop: Suppressing domain-sensitive channels for
601 domain generalization. In *Proceedings of the IEEE/CVF international conference on computer*
602 *vision*, pp. 19114–19124, 2023.

603

604 Kaiming He, Xiangyu Zhang, Shaoqing Ren, and Jian Sun. Deep residual learning for image
605 recognition. In *Proceedings of the IEEE conference on computer vision and pattern recognition*,
606 pp. 770–778, 2016.

607

608 Geoffrey Hinton, Oriol Vinyals, and Jeff Dean. Distilling the knowledge in a neural network. *arXiv*
609 *preprint arXiv:1503.02531*, 2015.

610

611 Edward J Hu, Yelong Shen, Phillip Wallis, Zeyuan Allen-Zhu, Yuanzhi Li, Shean Wang, Lu Wang,
612 Weizhu Chen, et al. Lora: Low-rank adaptation of large language models. *ICLR*, 1(2):3, 2022.

613

614 Zeyi Huang, Andy Zhou, Zijian Ling, Mu Cai, Haohan Wang, and Yong Jae Lee. A sentence speaks
615 a thousand images: Domain generalization through distilling clip with language guidance. In
616 *Proceedings of the IEEE/CVF International Conference on Computer Vision*, pp. 11685–11695,
617 2023.

618

619 Eyke Hüllermeier and Willem Waegeman. Aleatoric and epistemic uncertainty in machine learning:
620 An introduction to concepts and methods. *Machine Learning*, 110:457–506, 2021.

621

622 Taejong Joo, Uijung Chung, and Min-Gwan Seo. Being bayesian about categorical probability. In
623 *International conference on machine learning*, pp. 4950–4961. PMLR, 2020.

624

625 Daehee Kim, Youngjun Yoo, Seunghyun Park, Jinkyu Kim, and Jaekoo Lee. Selfreg: Self-supervised
626 contrastive regularization for domain generalization. In *Proceedings of the IEEE/CVF International*
627 *Conference on Computer Vision*, pp. 9619–9628, 2021.

628

629 Diederik P Kingma and Jimmy Ba. Adam: A method for stochastic optimization. *arXiv preprint*
630 *arXiv:1412.6980*, 2014.

631

632 Balaji Lakshminarayanan, Alexander Pritzel, and Charles Blundell. Simple and scalable predictive
633 uncertainty estimation using deep ensembles. *Advances in neural information processing systems*,
634 30, 2017.

635

636 Kyungmoon Lee, Sungyeon Kim, and Suha Kwak. Cross-domain ensemble distillation for domain
637 generalization. In *European Conference on Computer Vision*, pp. 1–20. Springer, 2022.

638

639 Da Li, Yongxin Yang, Yi-Zhe Song, and Timothy M Hospedales. Deeper, broader and artier domain
640 generalization. In *Proceedings of the IEEE international conference on computer vision*, pp.
641 5542–5550, 2017.

642

643 Da Li, Yongxin Yang, Yi-Zhe Song, and Timothy Hospedales. Learning to generalize: Meta-learning
644 for domain generalization. In *Proceedings of the AAAI conference on artificial intelligence*,
645 volume 32, 2018a.

646

647 Haoliang Li, Sinno Jialin Pan, Shiqi Wang, and Alex C Kot. Domain generalization with adversarial
648 feature learning. In *Proceedings of the IEEE conference on computer vision and pattern recognition*,
649 pp. 5400–5409, 2018b.

650

651 Tsung-Yi Lin, Priya Goyal, Ross Girshick, Kaiming He, and Piotr Dollár. Focal loss for dense object
652 detection. In *Proceedings of the IEEE international conference on computer vision*, pp. 2980–2988,
653 2017.

654

655 Yingnan Liu, Yingtian Zou, Rui Qiao, Fusheng Liu, Mong Li Lee, and Wynne Hsu. Cross-domain
656 feature augmentation for domain generalization. *arXiv preprint arXiv:2405.08586*, 2024.

648 Divyat Mahajan, Shruti Tople, and Amit Sharma. Domain generalization using causal matching. In
 649 *International Conference on Machine Learning*, pp. 7313–7324. PMLR, 2021.
 650

651 Andrey Malinin and Mark Gales. Predictive uncertainty estimation via prior networks. *Advances in*
 652 *neural information processing systems*, 31, 2018.

653 Andrey Malinin, Bruno Mlosozeniec, and Mark Gales. Ensemble distribution distillation. *arXiv*
 654 *preprint arXiv:1905.00076*, 2019.
 655

656 Udit Maniyar, Aniket Anand Deshmukh, Urun Dogan, Vineeth N Balasubramanian, et al. Zero shot
 657 domain generalization. *arXiv preprint arXiv:2008.07443*, 2020.

658 Jose G Moreno-Torres, Troy Raeder, Rocío Alaiz-Rodríguez, Nitesh V Chawla, and Francisco
 659 Herrera. A unifying view on dataset shift in classification. *Pattern recognition*, 45(1):521–530,
 660 2012.

661 Giung Nam, Jongmin Yoon, Yoonho Lee, and Juho Lee. Diversity matters when learning from
 662 ensembles. *Advances in neural information processing systems*, 34:8367–8377, 2021a.
 663

664 Hyeonseob Nam, HyunJae Lee, Jongchan Park, Wonjun Yoon, and Donggeun Yoo. Reducing domain
 665 gap by reducing style bias. In *Proceedings of the IEEE/CVF Conference on Computer Vision and*
 666 *Pattern Recognition*, pp. 8690–8699, 2021b.
 667

668 Ziwei Niu, Junkun Yuan, Xu Ma, Yingying Xu, Jing Liu, Yen-Wei Chen, Ruofeng Tong, and
 669 Lanfen Lin. Knowledge distillation-based domain-invariant representation learning for domain
 670 generalization. *IEEE Transactions on Multimedia*, 2023.

671 David Opitz and Richard Maclin. Popular ensemble methods: An empirical study. *Journal of*
 672 *artificial intelligence research*, 11:169–198, 1999.

673 Yaniv Ovadia, Emily Fertig, Jie Ren, Zachary Nado, David Sculley, Sebastian Nowozin, Joshua
 674 Dillon, Balaji Lakshminarayanan, and Jasper Snoek. Can you trust your model’s uncertainty?
 675 evaluating predictive uncertainty under dataset shift. *Advances in neural information processing*
 676 *systems*, 32, 2019.
 677

678 Xingchao Peng, Qinxun Bai, Xide Xia, Zijun Huang, Kate Saenko, and Bo Wang. Moment matching
 679 for multi-source domain adaptation. In *Proceedings of the IEEE/CVF international conference on*
 680 *computer vision*, pp. 1406–1415, 2019.
 681

682 Jonas Pfeiffer, Aishwarya Kamath, Andreas Rücklé, Kyunghyun Cho, and Iryna Gurevych. Adapter-
 683 fusion: Non-destructive task composition for transfer learning. In *Proceedings of the 16th*
 684 *conference of the European chapter of the association for computational linguistics: main volume*,
 685 pp. 487–503, 2021.

686 Alexandre Rame, Matthieu Kirchmeyer, Thibaud Rahier, Alain Rakotomamonjy, Patrick Gallinari,
 687 and Matthieu Cord. Diverse weight averaging for out-of-distribution generalization. *Advances in*
 688 *Neural Information Processing Systems*, 35:10821–10836, 2022.

689 Lior Rokach. Ensemble-based classifiers. *Artificial intelligence review*, 33:1–39, 2010.

690

691 Max Ryabinin, Andrey Malinin, and Mark Gales. Scaling ensemble distribution distillation to many
 692 classes with proxy targets. *Advances in Neural Information Processing Systems*, 34:6023–6035,
 693 2021.

694

695 John S Schreck, David John Gagne, Charlie Becker, William E Chapman, Kim Elmore, Da Fan,
 696 Gabrielle Gantos, Eliot Kim, Dhamma Kimpara, Thomas Martin, et al. Evidential deep learning:
 697 Enhancing predictive uncertainty estimation for earth system science applications. *Artificial*
 698 *Intelligence for the Earth Systems*, 3(4):230093, 2024.

699

700 Shiv Shankar, Vihari Piratla, Soumen Chakrabarti, Siddhartha Chaudhuri, Preethi Jyothi, and
 701 Sunita Sarawagi. Generalizing across domains via cross-gradient training. *arXiv preprint*
 702 *arXiv:1804.10745*, 2018.

702 Yuge Shi, Jeffrey Seely, Philip HS Torr, N Siddharth, Awni Hannun, Nicolas Usunier, and Gabriel
 703 Synnaeve. Gradient matching for domain generalization. *arXiv preprint arXiv:2104.09937*, 2021.
 704

705 Baochen Sun and Kate Saenko. Deep coral: Correlation alignment for deep domain adaptation. In
 706 *Computer Vision–ECCV 2016 Workshops: Amsterdam, The Netherlands, October 8–10 and 15–16,*
 707 *2016, Proceedings, Part III 14*, pp. 443–450. Springer, 2016.

708 Christian Szegedy, Vincent Vanhoucke, Sergey Ioffe, Jon Shlens, and Zbigniew Wojna. Rethinking
 709 the inception architecture for computer vision. In *Proceedings of the IEEE conference on computer*
 710 *vision and pattern recognition*, pp. 2818–2826, 2016.

711

712 Zhaorui Tan, Xi Yang, and Kaizhu Huang. Rethinking multi-domain generalization with a general
 713 learning objective. In *Proceedings of the IEEE/CVF Conference on Computer Vision and Pattern*
 714 *Recognition*, pp. 23512–23522, 2024.

715 Gemini Team, Rohan Anil, Sebastian Borgeaud, Jean-Baptiste Alayrac, Jiahui Yu, Radu Soricut,
 716 Johan Schalkwyk, Andrew M Dai, Anja Hauth, Katie Millican, et al. Gemini: a family of highly
 717 capable multimodal models. *arXiv preprint arXiv:2312.11805*, 2023.

718

719 Linh Tran, Bastiaan S Veeling, Kevin Roth, Jakub Swiatkowski, Joshua V Dillon, Jasper Snoek,
 720 Stephan Mandt, Tim Salimans, Sebastian Nowozin, and Rodolphe Jenatton. Hydra: Preserving
 721 ensemble diversity for model distillation. *arXiv preprint arXiv:2001.04694*, 2020.

722

723 Theodoros Tsiligkaridis. Information robust dirichlet networks for predictive uncertainty estimation,
 724 April 8 2021. US Patent App. 17/064,046.

725

726 Vladimir Vapnik. *The nature of statistical learning theory*. Springer science & business media, 1999.

727

728 Hemanth Venkateswara, Jose Eusebio, Shayok Chakraborty, and Sethuraman Panchanathan. Deep
 729 hashing network for unsupervised domain adaptation. In *Proceedings of the IEEE conference on*
computer vision and pattern recognition, pp. 5018–5027, 2017.

730

731 Riccardo Volpi, Hongseok Namkoong, Ozan Sener, John C Duchi, Vittorio Murino, and Silvio
 732 Savarese. Generalizing to unseen domains via adversarial data augmentation. *Advances in neural*
information processing systems, 31, 2018.

733

734 Dongdong Wang, Jingyao Xu, Siyang Lu, Xiang Wei, and Liqiang Wang. Ensemble distillation
 735 for out-of-distribution detection. In *2023 IEEE 29th International Conference on Parallel and*
Distributed Systems (ICPADS), pp. 248–253. IEEE, 2023a.

736

737 Jindong Wang, Cuiling Lan, Chang Liu, Yidong Ouyang, Tao Qin, Wang Lu, Yiqiang Chen, Wenjun
 738 Zeng, and Philip Yu. Generalizing to unseen domains: A survey on domain generalization. *IEEE*
Transactions on Knowledge and Data Engineering, 2022.

739

740 Pengfei Wang, Zhaoxiang Zhang, Zhen Lei, and Lei Zhang. Sharpness-aware gradient matching
 741 for domain generalization. In *Proceedings of the IEEE/CVF Conference on Computer Vision and*
Pattern Recognition, pp. 3769–3778, 2023b.

741

742 Xiran Wang, Jian Zhang, Lei Qi, and Yinghuan Shi. Balanced direction from multifarious choices:
 743 Arithmetic meta-learning for domain generalization. In *Proceedings of the Computer Vision and*
Pattern Recognition Conference, pp. 30577–30587, 2025.

744

745 Yufei Wang, Haoliang Li, Lap-pui Chau, and Alex C Kot. Embracing the dark knowledge: Do-
 746 main generalization using regularized knowledge distillation. In *Proceedings of the 29th ACM*
international conference on multimedia, pp. 2595–2604, 2021.

747

748 Prateek Yadav, Derek Tam, Leshem Choshen, Colin A Raffel, and Mohit Bansal. Ties-merging:
 749 Resolving interference when merging models. *Advances in Neural Information Processing Systems*,
 750 36:7093–7115, 2023.

751

752 Hao Yan and Yuhong Guo. Context-aware self-adaptation for domain generalization. *arXiv preprint*
 753 *arXiv:2504.03064*, 2025.

756 Huaxiu Yao, Xinyu Yang, Xinyi Pan, Shengchao Liu, Pang Wei Koh, and Chelsea Finn. Improving
757 domain generalization with domain relations. *arXiv preprint arXiv:2302.02609*, 2023.

758
759 Hanlin Zhang, Yi-Fan Zhang, Weiyang Liu, Adrian Weller, Bernhard Schölkopf, and Eric P Xing.
760 Towards principled disentanglement for domain generalization. In *Proceedings of the IEEE/CVF*
761 *Conference on Computer Vision and Pattern Recognition*, pp. 8024–8034, 2022.

762 Kaiyang Zhou, Yongxin Yang, Timothy Hospedales, and Tao Xiang. Learning to generate novel
763 domains for domain generalization. In *Computer Vision–ECCV 2020: 16th European Conference,*
764 *Glasgow, UK, August 23–28, 2020, Proceedings, Part XVI 16*, pp. 561–578. Springer, 2020.

765
766 Kaiyang Zhou, Yongxin Yang, Yu Qiao, and Tao Xiang. Domain adaptive ensemble learning. *IEEE*
767 *Transactions on Image Processing*, 30:8008–8018, 2021.

768 Zhi-Hua Zhou, Jianxin Wu, and Wei Tang. Ensembling neural networks: many could be better than
769 all. *Artificial intelligence*, 137(1-2):239–263, 2002.

770

771

772

773

774

775

776

777

778

779

780

781

782

783

784

785

786

787

788

789

790

791

792

793

794

795

796

797

798

799

800

801

802

803

804

805

806

807

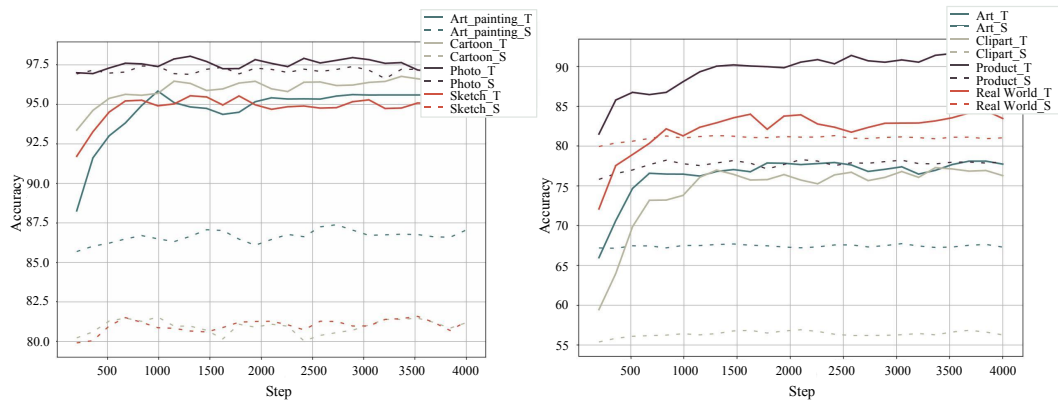
808

809

810 A COMPUTATIONAL COST ANALYSIS
811812 A.1 OVERHEAD OF TRAINING TEACHER MODELS
813

814 A key practical advantage of DomED is its computational efficiency, despite using an ensemble of
815 teacher models. This section demonstrates that the full training of teacher models is unnecessary
816 for effective distillation, which significantly reduces the method’s computational cost. As shown
817 in Figure 3, the distilled student models’ performance converges and stabilizes early in the training
818 process (within approximately 1,000 steps), long before the teacher models have fully converged on
819 their respective source domains. This observation indicates that while the guidance of teacher models
820 is essential, the student’s performance is not sensitive to the teachers’ final, fully converged state.

821 This observation significantly reduces the computational cost of our method. For a training set with
822 M domains, we can limit the training steps for each teacher to a fraction (e.g., $1/M$) of the steps
823 used for a standard single-model baseline.¹ Consequently, the total steps of training M teachers are
824 comparable to training a single model on all domains, making DomED a computationally practical
825 approach.



826
827
828
829
830
831
832
833
834
835
836
837
838
839 Figure 3: Impact of teacher training steps on student performance for (left) PACS and (right)
840 OfficeHome. Solid lines represent teacher accuracy on their source domain, while dashed lines show
841 the distilled student’s accuracy on the corresponding target domain. Note that student performance
842 (dashed lines) converges and stabilizes early, long before the teacher models (solid lines) have fully
843 converged.

844 A.2 TRAINING AND DISTILLATION COST
845846 Table 5: Computational cost and performance comparison on PACS (Target domain: Sketch).
847

Method	Wall-Time (h)	Peak Mem (GB) \downarrow	Acc. (%) \uparrow	ECE \downarrow	NLL \downarrow
ERM	1.91	8.13	79.3	0.121	0.919
DNA (Chu et al., 2022)	3.23	8.17	79.8	0.087	0.708
DomED	2.86	8.13	81.6	0.028	0.609
\hookrightarrow DomED (Teachers)	0.78	3.00	-	-	-
\hookrightarrow DomED (Student)	2.08	8.13	-	-	-

848 We provide a detailed computational cost analysis on PACS
849 in Table 5. The total training time for DomED is around 50%
850 longer than ERM while achieving significantly better accuracy
851 and calibration. The training of the teacher ensemble is partic-
852 ularly fast (0.78 h) and does not scale linearly with the number
853 of domains. This efficiency stems from two factors: 1) Since
854 each teacher sees only one domain, it is trained with a batch
855 size $1/M$ of the standard ERM batch size, reducing the cost of
856 each forward/backward pass. 2) As discussed in Appendix A.1, effective distillation does not require
857

858 Table 6: Total training time comparison
859 with SWAD on PACS (Target:
860 Sketch).
861

Method	Wall-Time(h) \downarrow
SWAD	2.41
DomED + SWAD	3.27

862
863 ¹According to the DomainBed protocol, the number of training steps is 5,000 for PACS, OfficeHome, VLCS,
TerraIncognita, and 15,000 for DomainNet.

864 fully converged teachers because the student model saturates early, which allows us to significantly
 865 reduce the number of teacher training steps compared to a standard run.
 866

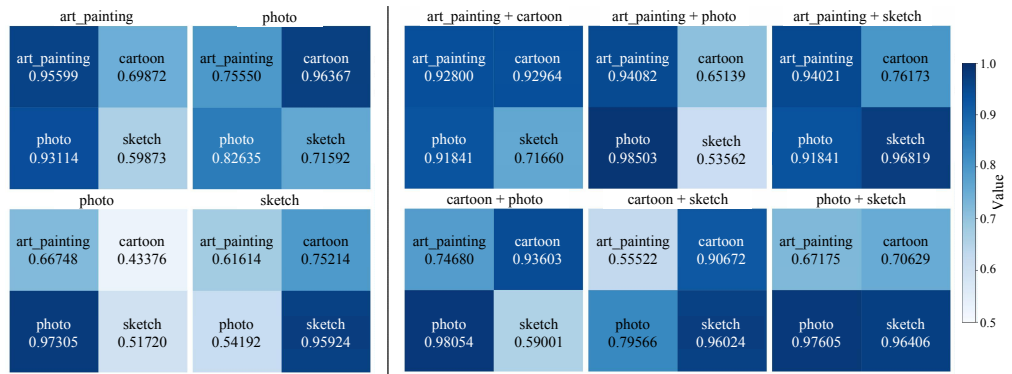
867 When combined with SWAD (Cha et al., 2021), we apply weight averaging only during the distillation
 868 phase of the student model. As shown in Table 6, this incurs a small overhead compared to standard
 869 SWAD, yet achieves higher accuracy by combining the benefits of ensemble knowledge and flat-
 870 minima optimization (See Table 2).
 871

B ANALYSIS OF TEACHER DIVERSITY

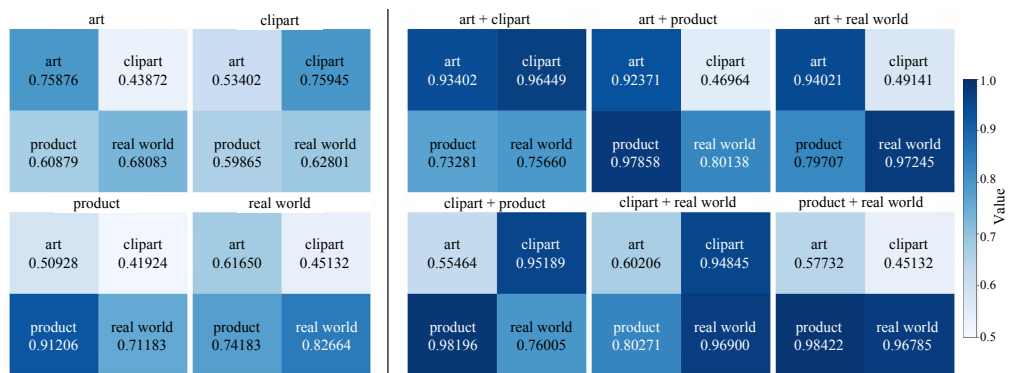
B.1 VISUALIZING TEACHER DIVERSITY

875 A central design principle of DomED is the use of a domain-specific data allocation scheme to foster
 876 the diversity required for effective ensemble learning. This section validates this strategy by visually
 877 analyzing the performance of teachers trained on distinct, single domains against those trained on
 878 dual-domain combinations. The accuracy heatmaps in Figures 4, 5, 6, and 7 visualize this comparison
 879 across the PACS, OfficeHome, VLCS, and TerraIncognita datasets, respectively.
 880

881 We observe a consistent pattern across these benchmarks where single-domain teachers (left panels)
 882 exhibit significantly higher specialization compared to their dual-domain counterparts (right panels).
 883 For instance, in the PACS dataset (Figure 4), a teacher trained exclusively on the “Art Painting” domain
 884 excels in its source domain but exhibits higher variance on others. In contrast, dual-domain teachers
 885 show more uniform performance across test domains. This empirical evidence supports our design
 886 choice: training each teacher on a single, distinct domain effectively encourages the development of
 887 specialized representations, which is a prerequisite for maximizing ensemble diversity.
 888



899 Figure 4: Accuracy heatmaps comparing single-domain (left) and dual-domain (right) teachers on
 900 the **PACS** dataset. Each block represents a trained teacher model, and each patch represents a test
 901 domain. The more varied color patterns on the left indicate higher specialization and diversity.
 902



915 Figure 5: Accuracy heatmaps for single-domain (left) and dual-domain (right) teachers trained on the
 916 **OfficeHome** dataset.
 917

The heatmaps further reveal how diversity varies across datasets. On the OfficeHome dataset
 (Figure 5), single-domain teachers maintain reasonable accuracy on unseen domains. This indicates

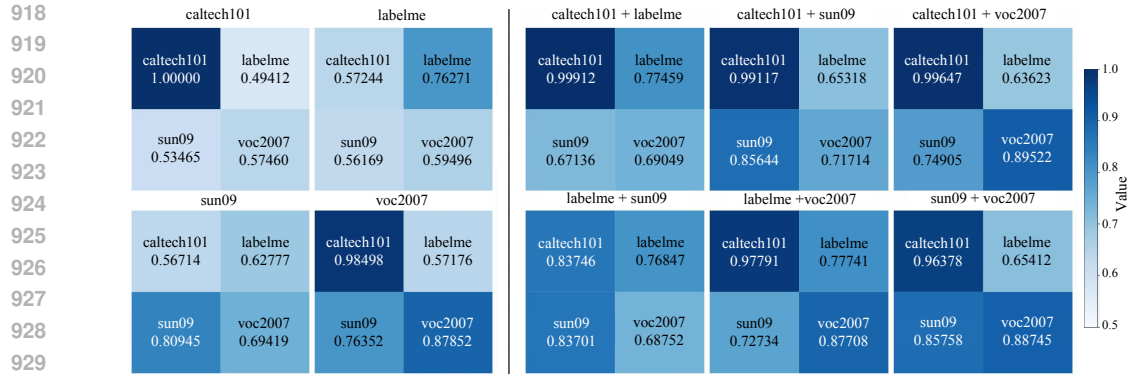


Figure 6: Accuracy heatmaps for single-domain (left) and dual-domain (right) teachers trained on the **VLCS** dataset.

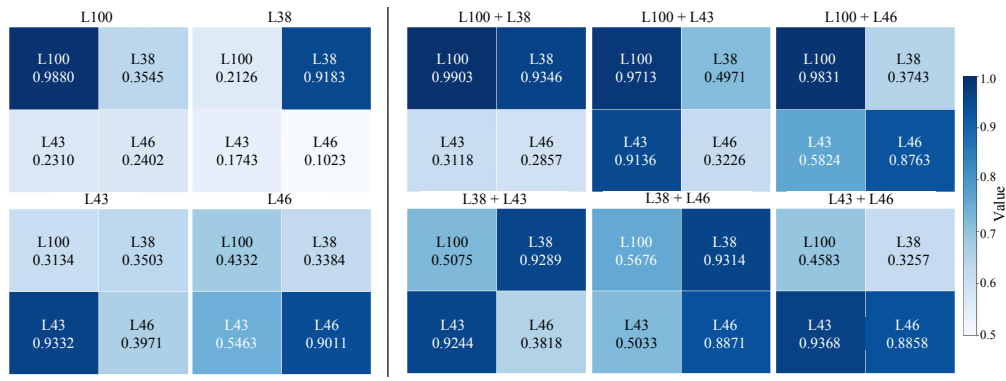


Figure 7: Accuracy heatmaps for single-domain (left) and dual-domain (right) teachers on the **TerraIncognita** dataset. Single-domain teachers exhibit high specialization.

that despite the stylistic differences between domains (e.g., Art, Product), the teachers successfully learn transferable semantic features that enable effective cross-domain generalization. In contrast, we observe a different behavior on the TerraIncognita dataset. As shown in Figure 7, single-domain teachers on TerraIncognita exhibit a distinct pattern of high specialization, achieving high accuracy on their respective source domains but suffering significant performance drops on unseen domains. We hypothesize that this behavior stems from the nature of camera trap data, where static backgrounds (e.g., specific vegetation or terrain) encourage models to learn domain-specific shortcuts that do not transfer well. Despite this challenging scenario where teacher transferability is limited, DomED effectively recovers useful signals to outperform the ERM baseline (50.2% vs. 47.8%).

B.2 IMPACT OF TEACHER DIVERSITY ON STUDENT PERFORMANCE

This section quantifies the impact of teacher diversity on student performance through a controlled experiment on the PACS dataset. We compared our proposed single-domain allocation strategy (high granularity, high diversity) against a dual-domain allocation baseline (low granularity, low diversity) where teachers are trained on pairs of domains. As presented in Table 7, the results demonstrate that the higher diversity provided by single-domain teachers translates into superior student performance. While accuracy improves by 2.0%, the impact on uncertainty is most notable: the single-domain strategy reduces ECE by over 50% (from 0.107 to 0.044) compared to the dual-domain baseline.

B.3 IMPACT OF ENSEMBLE SIZE ON STUDENT PERFORMANCE

Since our method ties the number of domain-specific teachers (or ensemble size) to that of training domains, varying the latter can affect teacher diversity as a result. To quantify the impact of ensemble size, we conducted an ablation study on the PACS dataset. We systematically train models on all possible 2-domain subsets ($M = 2$, each resulting in 2 domain-specific teachers) and compare their average performance against the standard 3-domain configuration ($M = 3$) as well as an ERM baseline trained on the same 2-domain subsets.

972
973
Table 7: Impact of teacher diversity: Comparison between single-domain (DomED) and dual-domain
allocation strategies on PACS.

974 975 976 977 978 979 980 981 982 983 984 985 986 987 988 989 990 991 992 993 994 995 996 997 998 999 Target Domain	974 975 976 977 978 979 980 981 982 983 984 985 986 987 988 989 990 991 992 993 994 995 996 997 998 999 Allocation	974 975 976 977 978 979 980 981 982 983 984 985 986 987 988 989 990 991 992 993 994 995 996 997 998 999 Diversity	974 975 976 977 978 979 980 981 982 983 984 985 986 987 988 989 990 991 992 993 994 995 996 997 998 999 Acc. (%) \uparrow	974 975 976 977 978 979 980 981 982 983 984 985 986 987 988 989 990 991 992 993 994 995 996 997 998 999 ECE \downarrow	974 975 976 977 978 979 980 981 982 983 984 985 986 987 988 989 990 991 992 993 994 995 996 997 998 999 NLL \downarrow	974 975 976 977 978 979 980 981 982 983 984 985 986 987 988 989 990 991 992 993 994 995 996 997 998 999 PRR \uparrow
974 975 976 977 978 979 980 981 982 983 984 985 986 987 988 989 990 991 992 993 994 995 996 997 998 999 Art Painting	974 975 976 977 978 979 980 981 982 983 984 985 986 987 988 989 990 991 992 993 994 995 996 997 998 999 Dual-domain Single-domain (DomED)	974 975 976 977 978 979 980 981 982 983 984 985 986 987 988 989 990 991 992 993 994 995 996 997 998 999 Low High	974 975 976 977 978 979 980 981 982 983 984 985 986 987 988 989 990 991 992 993 994 995 996 997 998 999 85.1 87.5	974 975 976 977 978 979 980 981 982 983 984 985 986 987 988 989 990 991 992 993 994 995 996 997 998 999 0.109 0.049	974 975 976 977 978 979 980 981 982 983 984 985 986 987 988 989 990 991 992 993 994 995 996 997 998 999 0.521 0.497	974 975 976 977 978 979 980 981 982 983 984 985 986 987 988 989 990 991 992 993 994 995 996 997 998 999 0.772 0.781
974 975 976 977 978 979 980 981 982 983 984 985 986 987 988 989 990 991 992 993 994 995 996 997 998 999 Cartoon	974 975 976 977 978 979 980 981 982 983 984 985 986 987 988 989 990 991 992 993 994 995 996 997 998 999 Dual-domain Single-domain (DomED)	974 975 976 977 978 979 980 981 982 983 984 985 986 987 988 989 990 991 992 993 994 995 996 997 998 999 Low High	974 975 976 977 978 979 980 981 982 983 984 985 986 987 988 989 990 991 992 993 994 995 996 997 998 999 78.3 81.5	974 975 976 977 978 979 980 981 982 983 984 985 986 987 988 989 990 991 992 993 994 995 996 997 998 999 0.076 0.038	974 975 976 977 978 979 980 981 982 983 984 985 986 987 988 989 990 991 992 993 994 995 996 997 998 999 0.726 0.628	974 975 976 977 978 979 980 981 982 983 984 985 986 987 988 989 990 991 992 993 994 995 996 997 998 999 0.654 0.738
974 975 976 977 978 979 980 981 982 983 984 985 986 987 988 989 990 991 992 993 994 995 996 997 998 999 Photo	974 975 976 977 978 979 980 981 982 983 984 985 986 987 988 989 990 991 992 993 994 995 996 997 998 999 Dual-domain Single-domain (DomED)	974 975 976 977 978 979 980 981 982 983 984 985 986 987 988 989 990 991 992 993 994 995 996 997 998 999 Low High	974 975 976 977 978 979 980 981 982 983 984 985 986 987 988 989 990 991 992 993 994 995 996 997 998 999 96.0 97.1	974 975 976 977 978 979 980 981 982 983 984 985 986 987 988 989 990 991 992 993 994 995 996 997 998 999 0.094 0.061	974 975 976 977 978 979 980 981 982 983 984 985 986 987 988 989 990 991 992 993 994 995 996 997 998 999 0.200 0.158	974 975 976 977 978 979 980 981 982 983 984 985 986 987 988 989 990 991 992 993 994 995 996 997 998 999 0.882 0.936
974 975 976 977 978 979 980 981 982 983 984 985 986 987 988 989 990 991 992 993 994 995 996 997 998 999 Sketch	974 975 976 977 978 979 980 981 982 983 984 985 986 987 988 989 990 991 992 993 994 995 996 997 998 999 Dual-domain Single-domain (DomED)	974 975 976 977 978 979 980 981 982 983 984 985 986 987 988 989 990 991 992 993 994 995 996 997 998 999 Low High	974 975 976 977 978 979 980 981 982 983 984 985 986 987 988 989 990 991 992 993 994 995 996 997 998 999 80.2 81.6	974 975 976 977 978 979 980 981 982 983 984 985 986 987 988 989 990 991 992 993 994 995 996 997 998 999 0.150 0.028	974 975 976 977 978 979 980 981 982 983 984 985 986 987 988 989 990 991 992 993 994 995 996 997 998 999 0.716 0.609	974 975 976 977 978 979 980 981 982 983 984 985 986 987 988 989 990 991 992 993 994 995 996 997 998 999 0.614 0.694
974 975 976 977 978 979 980 981 982 983 984 985 986 987 988 989 990 991 992 993 994 995 996 997 998 999 Average	974 975 976 977 978 979 980 981 982 983 984 985 986 987 988 989 990 991 992 993 994 995 996 997 998 999 Dual-domain Single-domain (DomED)	974 975 976 977 978 979 980 981 982 983 984 985 986 987 988 989 990 991 992 993 994 995 996 997 998 999 Low High	974 975 976 977 978 979 980 981 982 983 984 985 986 987 988 989 990 991 992 993 994 995 996 997 998 999 84.9 86.9	974 975 976 977 978 979 980 981 982 983 984 985 986 987 988 989 990 991 992 993 994 995 996 997 998 999 0.107 0.044	974 975 976 977 978 979 980 981 982 983 984 985 986 987 988 989 990 991 992 993 994 995 996 997 998 999 0.541 0.473	974 975 976 977 978 979 980 981 982 983 984 985 986 987 988 989 990 991 992 993 994 995 996 997 998 999 0.730 0.787

The results, summarized in Table 8, reveal that despite the reduction in teachers, DomED ($M = 2$) still outperforms the ERM baseline trained on the identical data subset. While accuracy is comparable, DomED maintains significantly better calibration (ECE 0.050 vs. 0.097). When compared to the full ensemble, reducing the size from 3 to 2 leads to a decrease in the Prediction Rejection Ratio (0.787 \rightarrow 0.701) and a slight increase in ECE. This confirms that the diversity provided by a larger set of domain experts is indeed a primary driver of high-quality uncertainty estimation. Crucially, the comparison indicates that while performance benefits from scaling up the number of domains, the method remains effective and robust when domain availability is limited.

C ROBUSTNESS TO WEAK TEACHERS

To evaluate the robustness of DomED against weak teachers trained on limited data, we performed a stress test on the PACS dataset, specifically using Sketch as the target domain. We simulated “amateur” teachers by reducing the training data of specific source domains (Art Painting, Photo, and Cartoon) to 50% and 25%. We compared our standard strategy (equal contribution) against a down-weighted strategy, where the weak teacher’s contribution to the soft target was manually suppressed (lowering the weight from 0.8 to 0.2).

As shown in Table 9, DomED proves to be remarkably resilient on the target domain. Even with only 25% of the training data, the performance drop is relatively small. Furthermore, manual down-weighting often degrades both accuracy and calibration (resulting in higher ECE). This suggests that even “amateur” teachers provide valuable diversity that aids generalization. The ensemble averaging mechanism, combined with the students hard-label loss anchor, naturally mitigates the noise from weaker teachers without requiring manual intervention.

D DARK KNOWLEDGE RETENTION

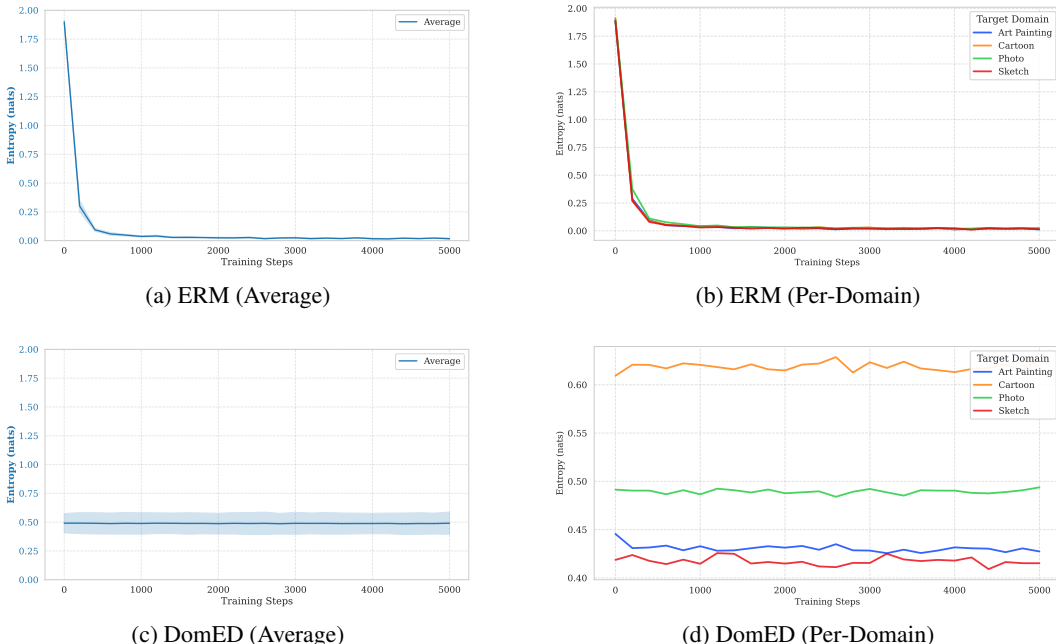
The preservation of “dark knowledge”, the rich information contained in the non-target class probabilities, is essential for effective knowledge distillation (Hinton et al., 2015). However, this information is often lost when models become overly confident during training. We investigated this phenomenon by tracking the entropy of a model’s predictive distribution (i.e. a categorical distribution) on the PACS dataset throughout the training process. For the student model of DomED, we track the entropy of its mean predictive distribution.

In standard knowledge distillation settings, where teachers predict on their training data, confidence typically peaks early, leading to a rapid collapse in entropy (Figure 8(a) and (b)). However, the experiment reveals a fundamentally different behavior for DomED (Figure 8(c) and (d)). Since our complementary distillation strategy requires teachers to generate predictions for domains they have never seen during training, they are effectively performing OOD inference. Consequently, they naturally yield “softer” probability distributions with stable, elevated entropy (≈ 0.49 nats on average) throughout the entire training process.

1026 Table 9: Robustness of different weighting strategies to data scarcity evaluated on PACS (Target
 1027 domain: Sketch).

Data-Scarce Domain	Data %	Strategy	Student Acc (%) \uparrow	ECE \downarrow	NLL \downarrow
<i>None (Baseline)</i>	100%	Standard	81.6 ± 0.2	0.028	0.609
Art Painting	50%	Standard	81.4 ± 0.3	0.042	0.597
	25%	Down-weighted	80.8 ± 0.2	0.049	0.614
	25%	Standard	80.5 ± 0.4	0.050	0.605
Photo	50%	Down-weighted	80.6 ± 0.3	0.061	0.626
	50%	Standard	79.8 ± 0.3	0.054	0.618
	25%	Down-weighted	80.2 ± 0.2	0.064	0.605
Cartoon	50%	Standard	78.0 ± 0.5	0.041	0.686
	25%	Down-weighted	76.5 ± 0.4	0.069	0.711
	25%	Standard	77.8 ± 0.3	0.029	0.671
	50%	Down-weighted	77.5 ± 0.2	0.027	0.703
	25%	Standard	78.6 ± 0.4	0.041	0.645
	25%	Down-weighted	76.9 ± 0.3	0.035	0.738

1044 To further validate whether the retained dark knowledge is sufficient, we evaluated an intervention
 1045 strategy where we doubled the distillation temperature during the late training phase. We found that
 1046 this yielded no notable improvement in accuracy or calibration. This leads us to conclude that the
 1047 natural “OOD signal” provided by the complementary allocation is already sufficient to preserve dark
 1048 knowledge, rendering additional entropy-preserving constraints unnecessary in our framework.



1070 Figure 8: Entropy of the predictive distribution during model training. The average entropy (a) and
 1071 per-domain entropy (b) of ERM rapidly collapse during training. In contrast, the average entropy (c)
 1072 and per-domain entropy (d) of the DomED student remains stable at a high level throughout training
 1073 (distillation).

E ABLATION ON LOSS COMPONENTS

1078 We conduct an ablation study on the components of our proposed loss function, $\mathcal{L}'_S = \mathcal{L}_S + \beta \mathcal{L}_{\text{Dir}}$,
 1079 to validate our decoupled distillation approach. This analysis compares the performance when
 using only the standard distillation loss (\mathcal{L}_S), only the Dirichlet NLL loss (\mathcal{L}_{Dir}), and our complete

1080
 1081 decoupled loss. The results are presented in Table 10 (Right). Relying solely on \mathcal{L}_{Dir} leads to a
 1082 significant degradation in classification accuracy, which is consistent with the issue of penalizing
 1083 confident predictions. While \mathcal{L}_S alone provides a strong performance baseline, our complete loss,
 1084 $\mathcal{L}_S + \mathcal{L}_{\text{Dir}}$, consistently maintains or even slightly improves accuracy across multiple benchmarks.

1085 Table 10: Ablation study of the distillation loss
 1086 components on three benchmarks, reporting clas-
 1087 sification accuracy (%).

PACS						
Loss	Art P.	Cartoon	Photo	Sketch	Avg.	
Only \mathcal{L}_{Dir}	64.49	60.78	87.20	59.07	67.88	
Only \mathcal{L}_S	87.46	81.48	97.08	81.55	86.89	
$\mathcal{L}_{\text{Dir}} + \mathcal{L}_S$	87.52	81.51	97.10	81.64	86.94	
VLCS						
Loss	Caltech	LabelMe	SUN09	VOC07	Avg.	
Only \mathcal{L}_{Dir}	76.15	57.69	75.36	69.60	69.70	
Only \mathcal{L}_S	98.26	65.08	78.23	78.21	79.94	
$\mathcal{L}_{\text{Dir}} + \mathcal{L}_S$	98.51	65.31	78.42	78.40	80.14	
TerraIncognita						
Loss	Loc. 100	Loc. 38	Loc. 43	Loc. 46	Avg.	
Only \mathcal{L}_{Dir}	28.61	47.27	20.34	27.56	30.90	
Only \mathcal{L}_S	55.12	46.47	57.81	38.53	49.48	
$\mathcal{L}_{\text{Dir}} + \mathcal{L}_S$	55.31	47.55	59.76	35.55	49.54	

To verify whether this design effectively resolves the optimization conflict discussed in Section 2.3 (i.e., balancing mean prediction and uncertainty spread), we further evaluate accuracy and uncertainty metrics on the PACS dataset. As shown in Table 11, combining the two losses significantly improves both ECE and PRR compared to using \mathcal{L}_{Dir} alone. These empirical results confirm that \mathcal{L}_S is essential for anchoring the mean prediction, which in turn allows \mathcal{L}_{Dir} to focus primarily on shaping the distribution’s spread without compromising convergence.

Table 11: Impact of loss components on accuracy and uncertainty metrics evaluated on PACS.

Loss	Acc. \uparrow	ECE \downarrow	NLL \downarrow	PRR \uparrow	K.Unc \uparrow
Only \mathcal{L}_{Dir}	67.88	0.397	0.917	0.640	0.672
Only \mathcal{L}_S	86.89	0.080	0.542	0.771	0.719
$\mathcal{L}_{\text{Dir}} + \mathcal{L}_S$	86.94	0.044	0.473	0.787	0.723

F SENSITIVITY TO HYPERPARAMETERS

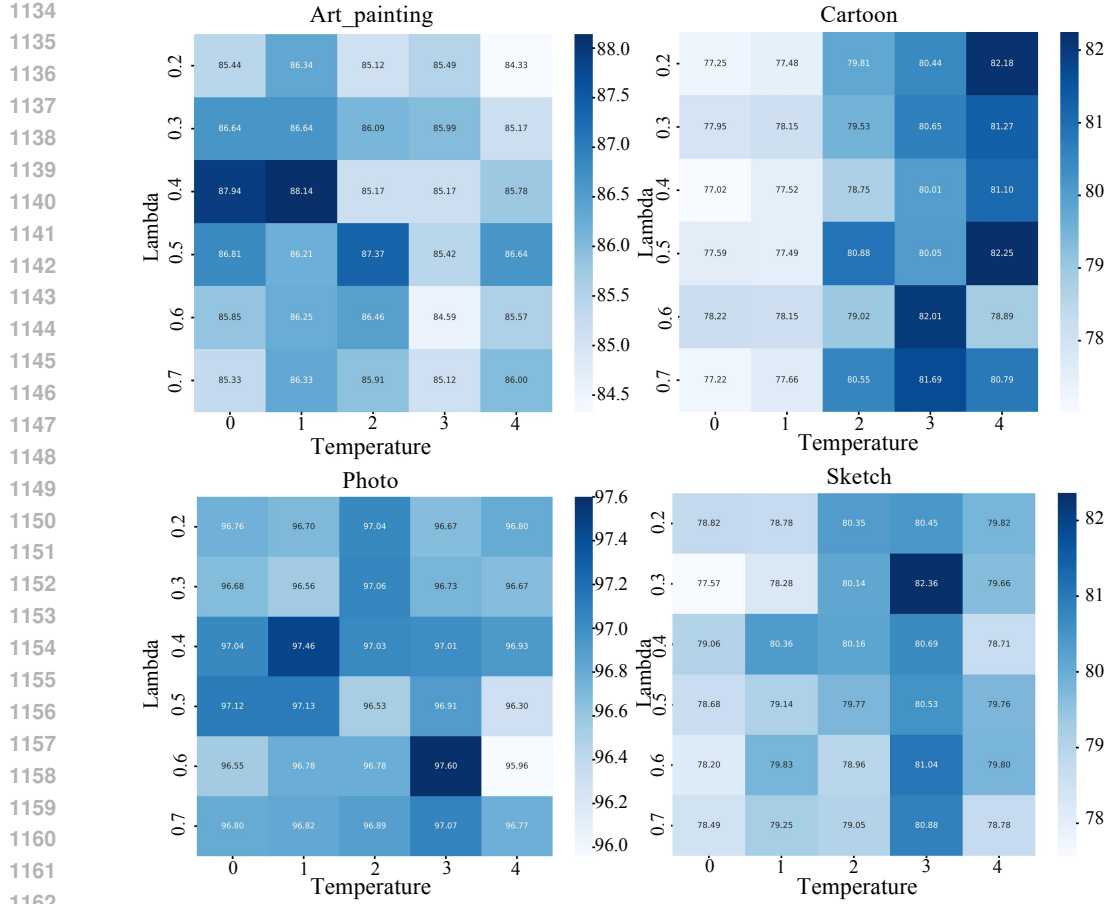
F.1 SOFT LABEL WEIGHT AND TEMPERATURE

We investigate the impact of the soft label weight (λ) and the temperature (τ) on model accuracy. Figures 9 and 10 present heatmaps of model performance on the PACS and VLCS datasets, respectively. The analysis shows that performance varies smoothly with these hyperparameters. For instance, on the PACS dataset, the Photo domain is least sensitive, while the Cartoon domain exhibits low sensitivity to changes in τ but high sensitivity to changes in λ . Overall, these results indicate that DomED’s performance is robust across a reasonable range of hyperparameter settings, validating the stability of our approach.

F.2 WEIGHT OF THE DIRICHLET NLL LOSS

The hyperparameter β in our decoupled distillation loss, $\mathcal{L}'_S = \mathcal{L}_S + \beta\mathcal{L}_{\text{Dir}}$, is crucial for balancing accuracy and uncertainty transfer. To analyze our method’s robustness to this hyperparameter, we investigate its impact on both the loss components and the final uncertainty estimates. As shown in Figure 11, we first examine the trade-off between the two loss components. Increasing β places more weight on the uncertainty-focused \mathcal{L}_{Dir} , causing its value to decrease at the expense of the accuracy-focused \mathcal{L}_S . The results indicate that a small value, such as $\beta = 0.01$, strikes an effective balance, allowing \mathcal{L}_{Dir} to converge sufficiently without significantly degrading the performance of \mathcal{L}_S .

This balance then translates directly to the final uncertainty estimates, as confirmed in Figure 12. The same region around $\beta = 0.01$ successfully preserves a high degree of both total and knowledge uncertainty from the ensemble. These results validate our core claim: the principled decoupling, controlled by a small β , effectively distills an ensemble’s uncertainty without the accuracy trade-off typically associated with relying solely on the Dirichlet NLL objective.

Figure 9: Test accuracies on PACS as λ and τ vary.

G COMPARISON WITH ALTERNATIVE CALIBRATION STRATEGIES

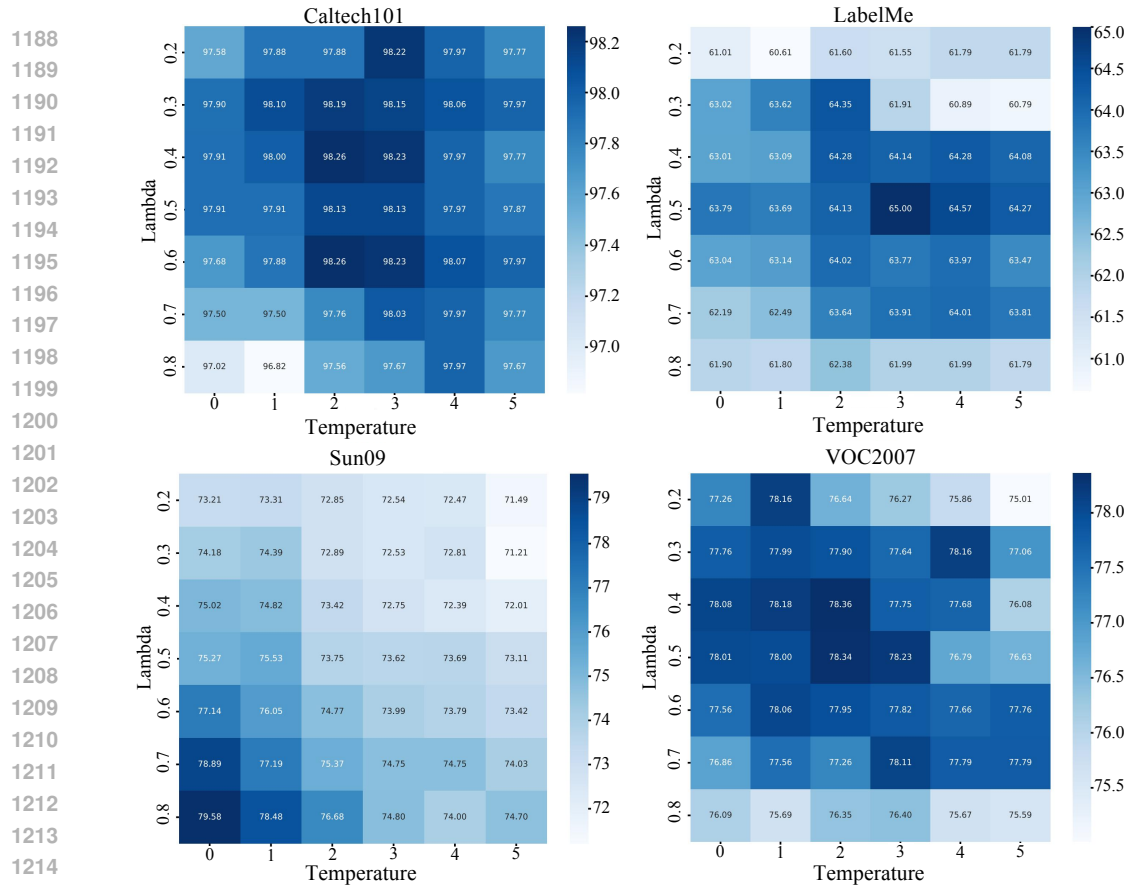
We evaluated DomED against Post-hoc Temperature Scaling (TS) (Guo et al., 2017), Label Smoothing (LS) (Szegedy et al., 2016), and Focal Loss (Lin et al., 2017) on the PACS dataset. The results are summarized in Table 12.

Table 12: Comparison of DomED with alternative calibration strategies on PACS. We evaluate Post-hoc Temperature Scaling (TS), Label Smoothing (LS, $\epsilon = 0.1$), and Focal Loss ($\gamma = 2.0$) within the same complementary allocation regime.

Category	Method / Configuration	ERR \downarrow	ECE \downarrow	NLL \downarrow	PRR \uparrow	OOD-AUC \uparrow
Baseline	\mathcal{L}_S only	0.1311	0.080	0.542	0.771	71.96
	+ Post-hoc TS (Guo et al., 2017)	0.1311	0.065	0.510	0.773	71.96
Alternatives	Label Smoothing (Szegedy et al., 2016)	0.1582	0.113	0.550	0.669	73.17
	Focal Loss (Lin et al., 2017)	0.1704	0.129	0.590	0.582	72.20
Ours	DomED ($\mathcal{L}_S + \mathcal{L}_{Dir}$) + Post-hoc TS	0.1306	0.044	0.473	0.787	72.25
		0.1306	0.105	0.580	0.785	72.26

Post-hoc TS reduces ECE but yields negligible gains in error detection (PRR) or OOD detection. While Label Smoothing achieves a high OOD-AUC, it incurs a performance trade-off, resulting in a 2.7% increase in classification error and a significantly higher ECE compared to DomED. Focal Loss similarly results in a higher error rate and worse calibration.

In contrast, DomED achieves the best balance with the lowest error (0.1306) and ECE (0.044) while maintaining the highest PRR (0.787). Notably, applying post-hoc TS to DomED degrades calibration, suggesting that our method learns intrinsically calibrated probabilities. We attribute this strong performance partly to the fact that the Dirichlet distribution is the conjugate prior of the categorical

Figure 10: Test accuracies on VLCS as λ and τ vary.

distribution. This makes it a theoretically natural choice for capturing the uncertainty inherent in an ensemble.

H ANALYSIS OF AN ALTERNATIVE DECOUPLING STRATEGY

The standard Dirichlet NLL loss (\mathcal{L}_{Dir}) can have a large gradient norm compared to the cross-entropy loss, which can destabilize training and harm classification accuracy. In the main paper, we address this with a simple and effective decoupled loss, $\mathcal{L}'_S = \mathcal{L}_S + \beta \mathcal{L}_{\text{Dir}}$. Here, we analyze a more complex alternative to provide further justification for our chosen design. The alternative strategy aims to directly isolate the learning of the mean prediction from the uncertainty. The mean of the Dirichlet distribution is given by $\mathbb{E}[\pi_c] = \alpha_c/\alpha_0 = e^{z_c}/\sum_k e^{z_k}$, which has the same form as the standard softmax function. The uncertainty, however, is controlled by the precision α_0 , which is determined by the sum of logits, $z_0 = \sum_c z_c$. This implies that z_0 introduces an extra degree of freedom for learning uncertainty. Therefore, we propose decoupling the uncertainty distillation by using Eq. 7 to learn z_0 and Eq. 5 to learn $\mathbb{E}[\pi_c]$. This ensures that the mean categorical distribution is learned regularly without compromising model accuracy. To achieve this, we reparameterize the z_c 's in Eq. 7 as follows:

$$z_c = \text{stop_gradient}(z_c - z_0) + z_0, \quad (9)$$

where $\text{stop_gradient}(\cdot)$ operation blocks gradients from directly flowing to z_c while allowing them to pass through z_0 .

However, our experiments showed this approach to be highly unstable. As illustrated in Figure 13, this reparameterization causes the Dirichlet NLL to diverge for all but a very narrow range of β . When β exceeds a small threshold (approximately 0.012), the model fails to converge, leading to a collapse in classification accuracy. This investigation highlights the difficulty of directly manipulating the gradients of the Dirichlet NLL via explicit reparameterization. It motivated our decision to use the simpler and far more robust decoupled loss function presented in the main paper, which

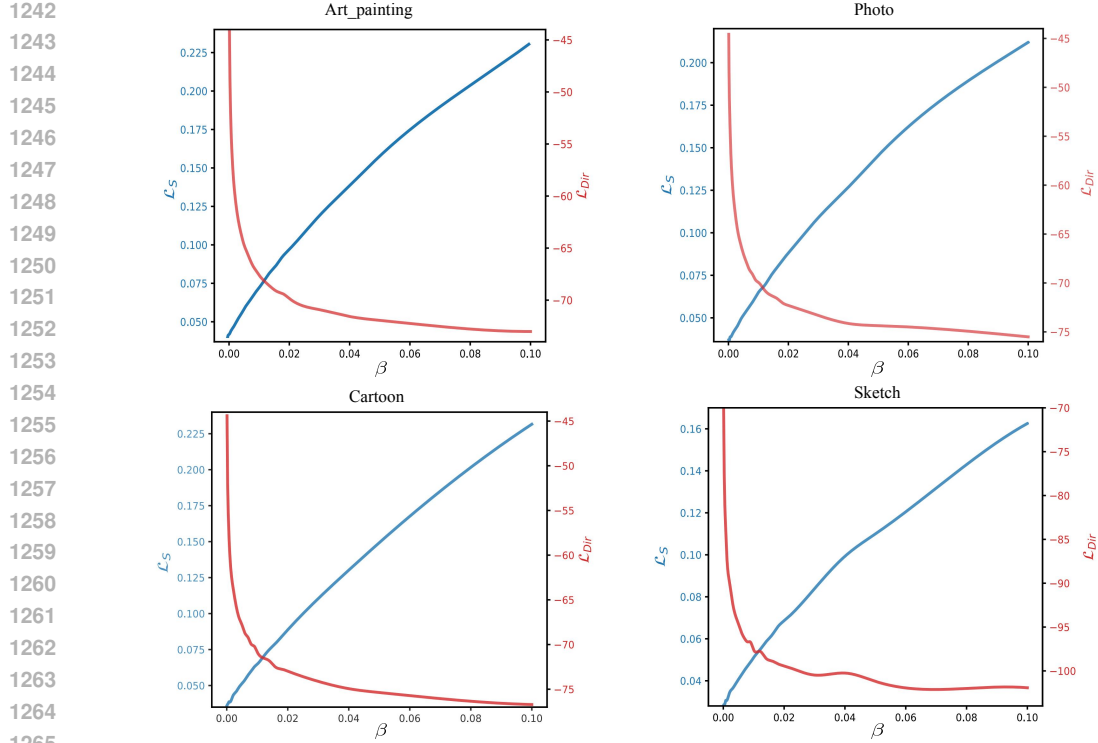


Figure 11: Converged values of the loss components \mathcal{L}_S (blue) and \mathcal{L}_{Dir} (red) as a function of β . The plot illustrates the trade-off between optimizing for accuracy (\mathcal{L}_S) and uncertainty (\mathcal{L}_{Dir}) on the PACS dataset.

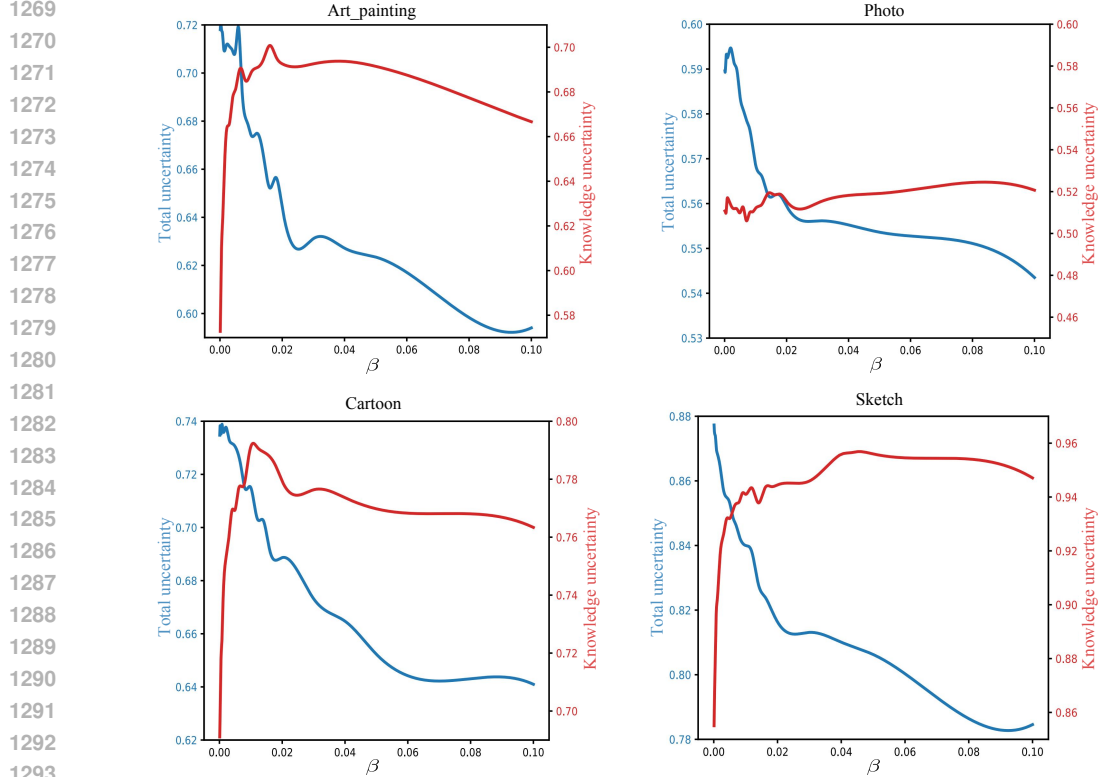


Figure 12: Impact of β on the final uncertainty estimates for the PACS dataset. The plots show that a small β (e.g., 0.01) is sufficient to distill a high degree of both total and knowledge uncertainty from the teacher ensemble.

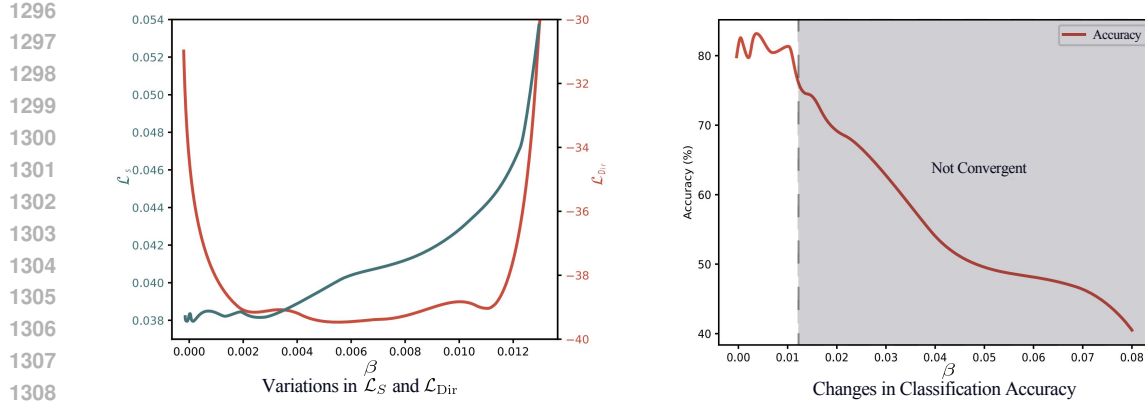


Figure 13: The alternative decoupling strategy using ‘stop_gradient’ is highly unstable. (Left) Both loss components, \mathcal{L}_S and \mathcal{L}_{Dir} , diverge with increasing β on the PACS dataset. (Right) Classification accuracy collapses when β exceeds a small threshold, indicating a failure to converge.

effectively balances the two objectives without requiring explicit gradient surgery and demonstrates stable performance across all benchmarks.

I ROBUSTNESS TO MODEL ARCHITECTURE

We evaluate the architectural robustness of DomED by repeating our experiments on the PACS dataset with a smaller CNN, ResNet-18 (He et al., 2016), and a Vision Transformer (ViT-B/16) (Dosovitskiy et al., 2021). As shown in Table 13, the results confirm that DomED is a broadly applicable framework that consistently improves upon the ERM baseline. With the smaller ResNet-18, DomED not only improves accuracy but also yields superior uncertainty estimates (ECE and NLL) compared to the full test-time ensemble, demonstrating its effectiveness on more compact models. The results on the ViT-B/16 are particularly compelling. Vision Transformers are known to struggle with generalization on smaller DG datasets, which is reflected in the high error rates of the ERM and ensemble baselines. In this challenging scenario, DomED provides a remarkable improvement, reducing the classification error by approximately 6 percentage points compared to the ensemble. This suggests that our distillation strategy may function as a powerful regularizer, validating DomED as a robust framework for diverse model families in the domain generalization setting.

Table 13: Performance on PACS across diverse model architectures (Arch.), including ResNet-18 (R-18) and the Vision Transformer Base model (ViT-B/16). DomED consistently improves accuracy and uncertainty estimation over the ERM baselines, demonstrating its robustness.

Arch. Model	ERR↓	ECE↓	NLL↓	PRR↑	T.Unc	K.Unc
ERM	0.192	0.128	0.895	0.775	0.723	-
R-18 Ensemble	0.172	0.066	0.697	0.772	0.724	0.698
DomED	0.175	0.043	0.579	0.745	0.713	0.729
ViT-B/16 Ensemble	0.211	0.155	0.988	0.688	0.723	-
DomED	0.146	0.079	0.534	0.785	0.623	0.692

reducing the classification error by approximately 6 percentage points compared to the ensemble. This suggests that our distillation strategy may function as a powerful regularizer, validating DomED as a robust framework for diverse model families in the domain generalization setting.

J ADDITIONAL RESULTS ON UNCERTAINTY QUANTIFICATION

This section provides a detailed breakdown of the uncertainty quantification results summarized in Section 3.3. We present the performance metrics for each leave-one-domain-out split, supplementing the averaged results shown in the main paper. Table 14 contains the per-domain calibration and reliability metrics corresponding to Table 3. Table 15 provides the per-domain OOD detection performance corresponding to Table 4.

Table 14: Detailed uncertainty quantification results on the PACS dataset. The table is split into two parts for better readability: Art Painting and Cartoon (top), Photo and Sketch (bottom). The best and second-best results are indicated by bold and underlined, respectively.

Model	Target: Art Painting				Target: Cartoon			
	ERR \downarrow	ECE \downarrow	NLL \downarrow	PRR \uparrow	ERR \downarrow	ECE \downarrow	NLL \downarrow	PRR \uparrow
Ensemble	0.139	0.026	0.489	0.830	0.160	0.057	0.633	0.761
EoA	0.111	0.048	0.375	0.894	0.143	0.099	0.627	0.774
ERM	0.152	0.065	0.496	0.808	0.200	0.125	0.821	0.731
Temp. Scaling	0.164	0.069	0.576	0.759	0.191	0.061	0.599	0.758
MC Drop (p=0.5)	0.163	0.100	0.686	0.772	0.238	0.189	1.414	0.678
MC Drop (p=0.1)	0.175	0.109	0.736	0.766	0.203	0.165	1.241	0.703
CORAL	0.139	0.071	0.514	0.670	<u>0.181</u>	0.117	0.754	0.484
EnD ²	0.274	0.131	1.262	0.142	0.481	0.358	2.590	0.007
DomED Teachers	0.269	0.080	0.847	0.657	0.401	0.074	1.456	0.386
Scheme (c)	0.128	<u>0.060</u>	<u>0.490</u>	<u>0.795</u>	0.190	<u>0.042</u>	0.698	0.679
Scheme (d)	0.125	0.125	0.477	0.748	0.179	0.053	0.697	0.710
DomED (Ours)	0.125	0.049	0.497	0.781	0.185	0.038	0.628	<u>0.738</u>
Target: Photo								
Model	ERR \downarrow	ECE \downarrow	NLL \downarrow	PRR \uparrow	ERR \downarrow	ECE \downarrow	NLL \downarrow	PRR \uparrow
	0.038	0.012	0.125	0.945	0.184	0.057	0.637	0.657
Ensemble	0.019	0.011	0.049	0.958	0.166	0.076	0.561	0.722
ERM	0.038	0.045	0.265	0.891	0.207	0.121	0.919	0.674
Temp. Scaling	0.037	0.018	0.147	0.902	0.197	0.045	0.626	0.672
MC Drop (p=0.5)	0.049	0.032	0.219	<u>0.904</u>	0.250	0.196	1.173	0.631
MC Drop (p=0.1)	0.059	0.044	0.290	0.881	0.191	0.131	0.754	0.726
CORAL	0.032	<u>0.026</u>	0.158	0.887	0.201	0.103	0.720	0.364
EnD ²	0.145	0.124	0.696	0.125	0.405	0.269	1.773	0.060
DomED Teachers	0.194	0.200	0.943	0.482	0.261	0.237	1.006	0.620
Scheme (c)	<u>0.030</u>	0.077	0.237	0.895	<u>0.186</u>	<u>0.038</u>	0.583	0.635
Scheme (d)	0.035	0.096	0.229	0.890	0.194	0.090	0.690	0.625
DomED (Ours)	0.029	0.061	<u>0.158</u>	0.936	0.184	0.028	<u>0.609</u>	<u>0.694</u>

Table 15: Out-of-distribution detection performance across four datasets, evaluated using the ROC-AUC metric. For each dataset, OOD samples are drawn from the test domain, while in-distribution (ID) samples are drawn from the train domains.

Model	PACS									
	Art Painting		Cartoon		Photo		Sketch		Avg.	
	T.Unc	K.Unc	T.Unc	K.Unc	T.Unc	K.Unc	T.Unc	K.Unc	T.Unc	K.Unc
ERM	0.73	—	0.69	—	0.57	—	0.89	—	0.71	—
Ensemble	0.75	0.71	0.73	0.76	0.54	0.46	0.90	0.91	0.73	0.71
DomED	0.69	0.72	0.72	0.77	0.57	0.47	0.84	0.93	0.71	0.72
OfficeHome										
Model	Art		Clipart		Product		Real World		Avg.	
	T.Unc	K.Unc	T.Unc	K.Unc	T.Unc	K.Unc	T.Unc	K.Unc	T.Unc	K.Unc
	0.72	—	0.79	—	0.62	—	0.57	—	0.67	—
ERM	0.75	0.65	0.81	0.84	0.63	0.68	0.58	0.65	0.69	0.70
Ensemble	0.69	0.71	0.72	0.79	0.51	0.66	0.50	0.64	0.60	0.70
VLCS										
Model	Caltech101		LabelMe		SUN09		VOC2007		Avg.	
	T.Unc	K.Unc	T.Unc	K.Unc	T.Unc	K.Unc	T.Unc	K.Unc	T.Unc	K.Unc
	0.32	—	0.43	—	0.66	—	0.65	—	0.51	—
ERM	0.33	0.23	0.45	0.51	0.67	0.72	0.66	0.71	0.53	0.54
Ensemble	0.48	0.51	0.44	0.58	0.69	0.83	0.67	0.85	0.57	0.69
TerraIncognita										
Model	Location 100		Location 38		Location 43		Location 46		Avg.	
	T.Unc	K.Unc	T.Unc	K.Unc	T.Unc	K.Unc	T.Unc	K.Unc	T.Unc	K.Unc
	0.74	—	0.70	—	0.76	—	0.79	—	0.75	—
ERM	0.79	0.80	0.76	0.87	0.74	0.60	0.85	0.90	0.78	0.79
Ensemble	0.75	0.66	0.74	0.86	0.74	0.60	0.83	0.87	0.77	0.75

1404 **K ETHICS STATEMENT**
14051406 This work focuses on foundational machine learning for domain generalization. All experiments
1407 were conducted on publicly available and widely used academic datasets (e.g., PACS, OfficeHome),
1408 which, to our knowledge, do not contain personally identifiable or sensitive content. Our research did
1409 not involve human subjects, and we do not foresee any direct negative societal impacts stemming
1410 from our methodology or findings.1411 **L REPRODUCIBILITY STATEMENT**
14121413 Our full implementation, built upon PyTorch and the DomainBed framework, is provided in the
1414 supplementary material. All experiments were conducted on NVIDIA V100 GPUs, following the
1415 standard data splits and evaluation protocols established by DomainBed. Key hyperparameters were
1416 selected using training-domain validation. A comprehensive list of hyperparameters and example
1417 execution commands are available in the supplementary material’s README file.
14181419 **M USE OF LARGE LANGUAGE MODELS**
14201421 We used Google’s Gemini 2.5 Pro (Team et al., 2023) to correct grammatical errors and refine the
1422 language in this manuscript. The model’s role was strictly that of a proofreading tool to improve
1423 clarity. All core scientific contributions, including research ideation, methodological development,
1424 experimental design, and the interpretation of results, were performed exclusively by the human
1425 authors.
1426
1427
1428
1429
1430
1431
1432
1433
1434
1435
1436
1437
1438
1439
1440
1441
1442
1443
1444
1445
1446
1447
1448
1449
1450
1451
1452
1453
1454
1455
1456
1457